Materials and Structures (2026) 59:363
https://doi.org/10.1617/s11527-026-03183-5

ORIGINAL ARTICLE

Durability assessment of bio-modified geopolymer concrete in simulated sewage environments

Mehrdad Ameri Vamkani · Zarina Yahya · Michaela Gkantou · Maria Ferentinou · Yangming Gao · Ana Bras

Received: 5 March 2026 / Revised: 16 June 2026 / Accepted: 24 June 2026 / Published online: 27 August 2026

Abstract Sewer infrastructure worldwide is ageing beyond its designed lifespan, rendering it increasingly vulnerable to biogenic sulphuric acid corrosion, cracking, and structural collapse. Geopolymer concrete represents a promising sustainable alternative to ordinary Portland cement in such aggressive environments; however, its durability under acidic conditions remains insufficiently characterised, particularly when combined with microbial modification. This study evaluated the sulphuric acid resistance and microstructural integrity of two fly ash-based geopolymer concrete formulations—a control mixture and a *Shewanella oneidensis* species-enhanced bio-modified mixture (Bio)—subjected to 1% H_2SO_4 immersion at 30 °C for 10 days to simulate sewer conditions. A multi-technique analytical framework comprising mechanical testing, capillary water absorption, SEM–EDS, XRF, FTIR, and XRD was employed to elucidate degradation mechanisms and quantify the effect of bacterial modification. Bio-modified specimens exhibited a denser, more homogeneous microstructure and markedly superior acid resistance, including an 82% increase in splitting tensile strength following acid exposure, in contrast to a 13% decrease recorded in control specimens. SEM–EDS analysis confirmed reduced cracking and enhanced retention of Ca and Fe in bio-modified specimens. XRD revealed the preservation of acid-resistant crystalline phases, including quartz and andradite, in bio-modified specimens, whereas the control specimens showed greater phase decomposition and decalcification. FTIR analysis indicated greater stability of Si–O–T bonds in bio-modified specimens, consistent with reduced silicate depolymerisation. These findings confirm that *Shewanella*-based bio-modification significantly enhances the durability of geopolymer concrete under sulphuric acid attack, supporting its application as a resilient and sustainable material for sewer infrastructure.

Keywords Bio-modification · *Shewanella*-enhanced · Geopolymer concrete · Acid resistance · Sewage infrastructure

M. Ameri Vamkani (✉) · M. Gkantou · M. Ferentinou · Y. Gao · A. Bras (✉)
Department of Built Environment, Built Environment and Sustainable Technologies (BEST) Research Institute, Liverpool John Moores University, Byrom Street, Liverpool L3 3AF, UK
e-mail: m.amerivamkani@ljmu.ac.uk

A. Bras
e-mail: a.m.armadabras@ljmu.ac.uk

M. Gkantou
e-mail: m.gkantou@ljmu.ac.uk

M. Ferentinou
e-mail: m.ferentinou@ljmu.ac.uk

Y. Gao
e-mail: y.gao@ljmu.ac.uk

Z. Yahya
Faculty of Civil Engineering & Technology, Universiti Malaysia Perlis (UniMAP), Perlis, Malaysia
e-mail: zarinayahya@unimap.edu.my

1 Introduction

As the demand for concrete structures increases, the need for sustainable alternatives to Ordinary Portland Cement (OPC) grows accordingly [1]. Geopolymer Concrete (GPC), produced through geopolymerisation, the binding of aluminosilicates with highly alkaline solutions, is an emerging class of cementitious material considered a next-generation solution for civil infrastructure. Researchers are increasingly exploring GPC using fly ash, blast furnace slag, and metakaolin, as well as industrial waste, additives, and microbes, to reduce the environmental impact of cement production [2], 3].

Geopolymer can present comparable properties to OPC [4]. It possesses a greater ability to withstand acid exposure and abrasive forces, along with reduced permeability. In wastewater sewage networks, the calcium-rich byproducts of OPC hydration are typically dissolved by acids, consequently rendering OPC susceptible to acid-induced corrosion [5, 6]. Typically, in wastewater networks employing OPC, corrosion arises from a two-stage process involving biogenic sulphate reduction and subsequent reoxidation [7]. This process begins when sulphate present in confined pipelines or stagnant water is transformed by anaerobic bacteria into hydrogen sulphide (H_2S) under oxygen-deprived conditions [8, 9]. Figure 1 schematically illustrates the two-stage biogenic corrosion mechanism in OPC-based sewer environments. In the first stage, sulphate-reducing bacteria in the submerged zone convert SO_4^{2-} to H_2S under anaerobic conditions. In the second stage, H_2S volatilises into the sewer headspace, where sulphur-oxidising bacteria oxidise it to H_2SO_4. This acid subsequently attacks calcium-bearing phases in the OPC matrix, causing progressive structural degradation [10].

According to Chen et al. [11], while GPC generally exhibits better sulphate resistance than OPC, the addition of 8% SO_4^{-2}increases the median pore size in geopolymer pastes, potentially increasing susceptibility to long-term corrosive attack, although erosion products may initially fill pores [12]. Despite some long-term in situ evidence [13], the durability of GPC under microbially induced acid corrosion requires further systematic investigation. Beyond durability, the practical application of GPC presents additional challenges. Alkali-activated fly ash geopolymer requires elevated energy input to activate polymerisation [14], and high concentrations of sodium or potassium hydroxide are necessary to achieve adequate mechanical strength [15]. Furthermore, curing at high temperatures (40–95 °C) accelerates geopolymerisation but increases energy consumption [16], and steam curing between 60 and 80 °C, while improving compressive strength, similarly incurs higher energy costs [17].

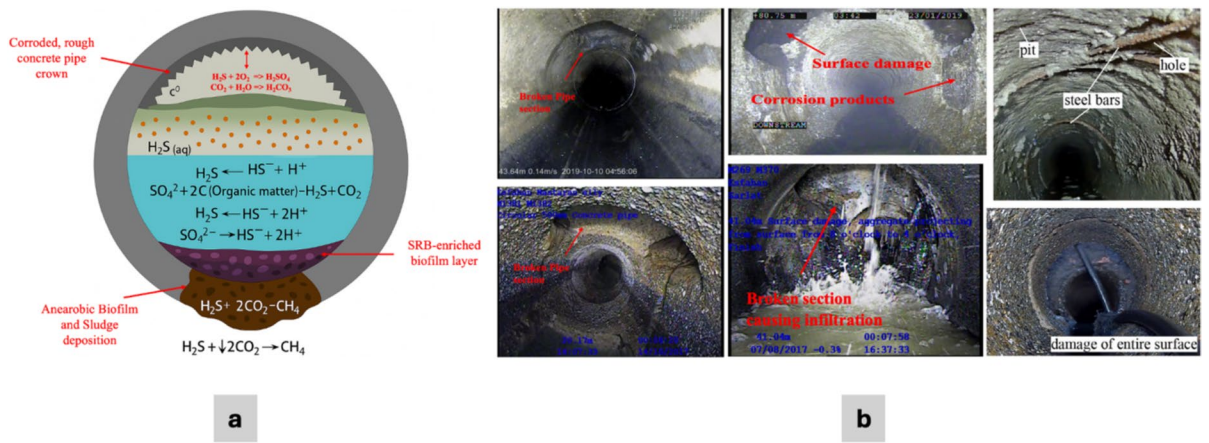

Fig. 1 **a** Schematic illustration of the two-stage biogenic corrosion mechanism in OPC-based sewer environments, showing sulphate reduction in the submerged zone and subsequent H_2SO_4 formation in the sewer crown; **b** field photographs showing structural damage on the inner surface of underground concrete pipes resulting from biogenic acid corrosion, including broken pipe sections, surface deterioration, corrosion products, aggregate exposure, infiltration, and full surface damage. All field photographs are original, taken from site inspections; all copyrights reserved

Biomineralisation, the biologically mediated precipitation of minerals within a material matrix, has emerged as a nature-inspired approach to consolidate, repair, and protect construction materials; Microbially Induced Calcium Carbonate Precipitation (MICP) is one such process, exploiting bacterial metabolism to deposit $CaCO_3$ and seal microcracks. In the MICP process, the metabolism of bacteria such as ureolytic Bacillus or iron-respiring *Shewanella* is exploited to promote calcium carbonate ($CaCO_3$) deposition in geopolymer concrete to seal microcracks [18]. Recent studies have demonstrated self-healing properties in various types of building materials, including conventional concrete, engineered cementitious composites (ECC), and engineered geopolymeric composites (EGC) [19–21].

Bacteria-based self-healing geopolymer concrete offers a compelling solution to increase the durability and longevity of concrete structures in sewage systems [22–24]. These challenges underscore the need for innovative materials capable of withstanding prolonged exposure to harsh wastewater and acidic conditions [25]. The ability of *Shewanella* genus to thrive in alkaline environments, inhibit corrosion, and sustain biomineralisation activity makes it a particularly suitable candidate for enhancing geopolymer performance in sewer systems [26]. Despite these promising initial findings, it is important to recognise that further studies are necessary to fully understand the performance of *Shewanella* species-based self-healing geopolymer concrete in real-world wastewater environments. The biological processes initiated by these bacteria not only fill cracks but also contribute to the overall durability of the material, making it more resilient to environmental stressors [27].

Previous studies have examined a range of topics, including the effect of fly ash ratios and alkaline activators on microstructure and dielectric properties [28, 29], and the self-healing behaviour of geopolymer composites in alkaline environments [30, 31], employing microscopic, mechanical, and chemical characterisation techniques.

For example, Zhao et al. [3] showed that repair products, including C(N)-A-S-H and calcium carbonate, can help improve self-healing in alkaline environments. The compounds used in these studies include fly ash, slag, GGBS (Ground Granulated Blast-Furnace Slag) and alkaline activators such as NaOH and KOH. These compounds not only help to improve the mechanical properties and durability of concrete but also play a key role in self-healing processes [32, 33]. The research results clearly show the positive effect of these compounds on the properties of geopolymer concretes, so Rihan et al. [34] emphasised that a high concentration of NaOH significantly increases compressive strength. Also, Guo et al. [1] presented positive results in the field of self-healing, which indicates the high potential of these materials in construction applications. However, there are also challenges, including the degradation of properties at high concentrations that Zhao et al. [3] mentioned. This issue shows the need for further research to optimise conditions and compounds. Wu et al. [35] investigated the self-healing performance of engineered geopolymer composites subjected to sodium sulphate. Sodium sulphate is a common corrosive agent in various environments, and while Wu et al. [35] focus on the effects of sodium sulphate, the present research specifically targets sulphuric acid, which is notorious for its aggressive nature in sewer systems.

Despite extensive literature on geopolymer composites, key research gaps persist. Most studies focus on healing in alkaline or neutral environments, with little attention to acidic conditions, especially simulating wastewater systems. While much research has explored Bacillus species [36], a significant gap exists in the literature that has examined *Shewanella* bacteria in fly ash-based geopolymers. The novelty of this study lies in emphasising biological compatibility and durability in acidic environments, aiding the development of resilient, sustainable materials. This research addresses the physico-mechanical and microstructural characteristics of geopolymer concrete, modified by Shewanella species, subjected to a high concentration of sulphuric acid exposure at 30 °C, simulating sewer environments. This evaluation employs a suite of techniques, including SEM–EDS, XRF, XRD, FTIR, and durability tests such as splitting tensile strength, water absorption via capillary and weight change observation.

2 Materials and sample preparation

2.1 Materials and mix design

The preparation of self-healing geopolymer concrete mixtures involved the use of fly ash (FA), coarse

aggregates, sand, sodium silicate, and sodium hydroxide serving as the alkaline activator. Fly ash, characterised by a measured calcium oxide (CaO) content of less than 10%, was selected to ensure its compatibility with geopolymerisation processes. The chemical composition of the fly ash was analysed using X-ray fluorescence (XRF) presented in Table 1, revealing a high content of silica (SiO_2) and alumina (Al_2O_3), which are crucial for the formation of a durable aluminosilicate network. This composition facilitates the development of a resilient aluminosilicate network during geopolymerisation, potentially improving its chemical durability [37].

Two distinct types of geopolymer mixtures were formulated:

(1) a control mixture and
(2) a bio-modified mixture that incorporated a bioproduct containing *Shewanella oneidensis*.

The introduction of the bioproduct occurred directly during the final mixing stage to mitigate mechanical stress on the bacterial cells. Shewanella oneidensis was selected for its distinctive capacity to withstand acidic, anoxic environments and to reduce Fe (III), thereby facilitating the formation of stable iron-silicate phases such as andradite. Its electron transport mechanisms and biomineralisation abilities support $CaCO_3$ precipitation and retention of structural ions, as evidenced by XRD, SEM–EDS, and FTIR analyses, rendering Shewanella oneidensis particularly suitable for improving acid resistance in geopolymer concretes used in sewer environments [38–40]. Regarding mix preparation, the alkaline activator was produced by dissolving sodium hydroxide (NaOH) pellets in distilled water at a concentration of 12 Molar, prepared 24 h prior to the experiment, and subsequently combined with sodium silicate (Na2SiO3) (1.5 S.G., d = 1.5 g/ml, S/6340/17; Fisher Chemical, UK). Sodium silicate with a specific gravity of 1.5 was supplied by Fisher Scientific. The coarse aggregate used was supplied by Specialist Aggregate and Travis Perkins, UK, with a size ranging from 10–20 mm. Sand as fine aggregates was obtained from Tarmac Plant, UK.

2.2 Specimen preparation

(i) *Geopolymer mix proportions*

The concrete mix design for six cubes (100 × 100 mm) and six cylinders (100 × 150 mm) consisted of 10.85 kg, 9.77 kg, 14.65 kg, 1.55 kg, and 3.88 kg of fly ash, sand, aggregate, NaOH solution, and sodium silicate solution, respectively. The ratios of fly ash to activator and NaOH to sodium silicate employed were 2.0 and 2.5, respectively.

(ii) *Preparation of the bacterial suspension*

This research utilised a strain of Shewanella supplied by a German company, and Tryptic Soy Broth (TSB) was used as a nutrient-rich medium to facilitate bacterial growth. TSB contain pancreatic digest of casein (17 g/L), papain digest of soybean meal (3.0 g/L), sodium chloride (5.0 g/l), dibasic potassium phosphate (2.5 g/L), and glucose (2.5 g/L). The Shewanella strain was transferred to TSB that had been sterilised using autoclaving at 121 °C for 20 min and subsequently cooled. Following that, the bacteria culture was placed in a shaking incubator for a duration of 19h at a temperature of 30℃ and a speed of 200 rpm in order to produce a liquid bacteria solution (bioproduct). Following incubation, the number of colonies was counted using the serial dilution technique, resulting in a colony-forming unit per millilitre (CFU/ml) of 10^8 CFU/ml in the bacteria solution.

(iii) *Preparation of geopolymer concrete mixtures*

The mixing process began with a 5-min dry mixing of fly ash, coarse aggregate, and sand at low speed, followed by a 3-min mixing with gradual addition of the alkaline activator. For bio-modified specimens, 200 mL of the bioproduct was added directly during the final

Table 1 Chemical compositions of fly ash (wt.%)

SiO_2	$Al2O_3$	Fe_2O_3	P_2O_5	SO_3	TiO_2	CaO	K_2O	MgO	SrO	BaO
56.3	20.8	5.53	0.836	0.578	0.915	3.33	1.99	1.53	0.16	0.154

mixing stage and mixed for an additional 2 min to mitigate mechanical stress on bacterial cells.

(iv) *Casting and specimen dimensions*
Two series of compositions were cast; for each, six cylinders (100 mm × 150 mm) were prepared. The 100 × 50 mm cylindrical specimens were selected for resource efficiency and compatibility with the acid immersion test rig, ensuring uniform acid exposure and consistent microstructural sampling [41].

(v) *Curing conditions*
Specimens were demoulded after 24h of curing at 20 °C, then cured for 7 days at 30 °C with a humidity of 60%. This curing method is critical for achieving optimal mechanical properties in fly ash-based geopolymer systems [42].

The present research aims to create a homogeneous geopolymer concrete that can be tested for its self-healing capabilities and mechanical properties, similar to the objectives of Naresh et al. (2024) [43].

2.3 Simulation of sewer conditions

The 1% H_2SO_4 solution was prepared by diluting sulphuric acid (assay 96.23%, d = 1.83 g/mL, analytical reagent grade, CAS 7664-93-9, Lot 2,666,820; Fisher Chemical, Loughborough, UK) with distilled water, following established laboratory procedures [44], to simulate sewer-like acidic conditions (pH of 1.26 and humidity of 60%) over 10 days, during which pH was periodically monitored with a calibrated meter. This accelerated test evaluated the inherent acid resistance of the geopolymer matrix and the initial impact of bacterial modification, allowing rapid comparison of degradation behaviours under controlled, highly aggressive conditions, consistent with previous studies on accelerated acid testing of cementitious and alkali-activated materials [45].

3 Methodology

The chemical immersion method was employed to assess the resistance of materials to sulphuric acid, simulating the conditions of a sewer environment for the specimens. Specifically, cylindrical specimens, 100 × 50 mm, were immersed in a 1% sulphuric acid solution at 28 days of age (at 30 °C and humidity of 60%) for a period of 10 days. It is important to note that, in this study, the term "healing" does not refer to traditional crack closure but instead to bacterial-induced densification of the matrix and stabilisation of its composition. Following immersion, all specimens were removed from the acid solutions and stored in an oven at 30 °C for another 24h prior to testing. The testing procedures are as follows:

3.1 3.1. Compressive strength

The compressive strength was determined in accordance with BS EN 12390-3:2009, with the average of 6 cubic specimens calculated and reported in this study to establish their baseline mechanical properties before acid exposure.

3.2 3.2. Visual observation

Surface photographs of each specimen were taken every 4 days during the 10-day acid exposure period to monitor visible signs of degradation. Observations focused on changes such as surface discolouration, white deposit formation, surface softening, and any visible cracking or scaling. Close-up examination of surface deposits was conducted using a Nikon SMZ25 stereo microscope equipped with a C-HGFI INTENSILIGHT HG precentred fibre illuminator; images were captured using NIS-Elements software (v5.21.03).

3.3 3.3. Weight change

Variations in sample mass (immersed in acid) were recorded every 4 days to evaluate the extent of material degradation due to acid exposure.

3.4 3.4. Water absorption via capillary

Water absorption by capillarity was tested following BS EN 1015-18:2002 guidelines. Cylinder specimens measuring 50 mm thick and 100 mm in diameter were used. Three specimens of each type were dried in an oven at 30 °C until their mass changed by no more than 0.1%. Subsequently, the cylindrical specimens

were submerged in 10 mm of water inside a sealed container to ensure a stable hydrothermal environment. The specimens' mass was recorded at 0, 5, 15, 30 min, 1, 2, 3h, then at 21h, 24h, and up to 28 days, or until water absorption stabilised.

3.5 3.5. Splitting tensile strength

Splitting tensile strength for both control and healing specimens (ASTM C496), was conducted after a 10-day exposure period for both the control and bio-modified specimens (3 specimens of each). All specimens, including those exposed to the acid, were subsequently placed in an oven at a temperature of 30 °C for 24h to ensure uniform moisture content prior to testing.

3.6 3.6. Microstructural analysis

3.6.1 3.6.1. Sample preparation

For XRF, XRD, and FTIR analyses, fragments recovered from compressive strength testing were ground into a fine powder using an agate mortar and pestle prior to analysis.

3.6.2 3.6.2. X-ray fluorescence (XRF)

Ground powder samples were analysed using a Rigaku NEX CG II XRF spectrometer to determine the chemical composition of each mix design. Three specimens per mix were tested, and average values were recorded.

3.6.3 X-ray diffraction (XRD)

Phase changes and crystalline degradation under acidic conditions were investigated using a Rigaku MiniFlex powder X-ray diffractometer, scanning over an angular range of 5–90° at a scan rate of 0.01° per second.

3.6.4 Fourier transform infrared spectroscopy (FTIR)

Ground powder samples were analysed using an Agilent Cary 630 FTIR system, within a spectral range of 500–4000 cm^{-1}, to assess chemical bonding environments and changes in molecular structure resulting from acid exposure.

3.6.5 Scanning electron microscopy and energy dispersive X-ray spectroscopy (SEM–EDS)

Specimens were sectioned to expose both core and surface regions, then crushed and gold-coated prior to examination. Microstructural analysis was performed using an FEI Inspect S scanning electron microscope at 0.1–30 kV, using backscattered electron (BSE) imaging for microstructural characterisation and secondary electron (SE) imaging for surface topography. Elemental composition was determined via EDS at six spots per fragment on both acid-exposed and unexposed control and bio-modified specimens at 28 days. An additional SEM scan was conducted at 180 days to assess bacterial survival and evaluate the long-term microstructural influence of bio-modification within the geopolymer matrix.

4 Results and discussions

4.1 Compressive strength

Figure 2 shows that both mixes reached similar 28-day strengths expected for low-Ca fly ash GPC [46], with the bio-modified sample at 35.92 MPa and the control at 35.23 MPa. The roughly 2% increase in the bio-modified mix falls within measurement error margins (see error bars), suggesting that adding the bacterial component does not negatively impact geopolymerisation or early mechanical properties. Coefficients of variation (COV) below 30% for all measurements. The calculated COV for the datasets confirms a high level of experimental consistency and reliability of the reported results.

This baseline matches microstructural analyses, discussed in detail in later sections, which display a denser, more continuous gel in bio-modified specimens and fewer cracks. These 28-day results thus provide a reference for assessing changes following acid exposure, where observed differences are mainly due to transport mechanisms and microstructural features rather than initial strength differences.

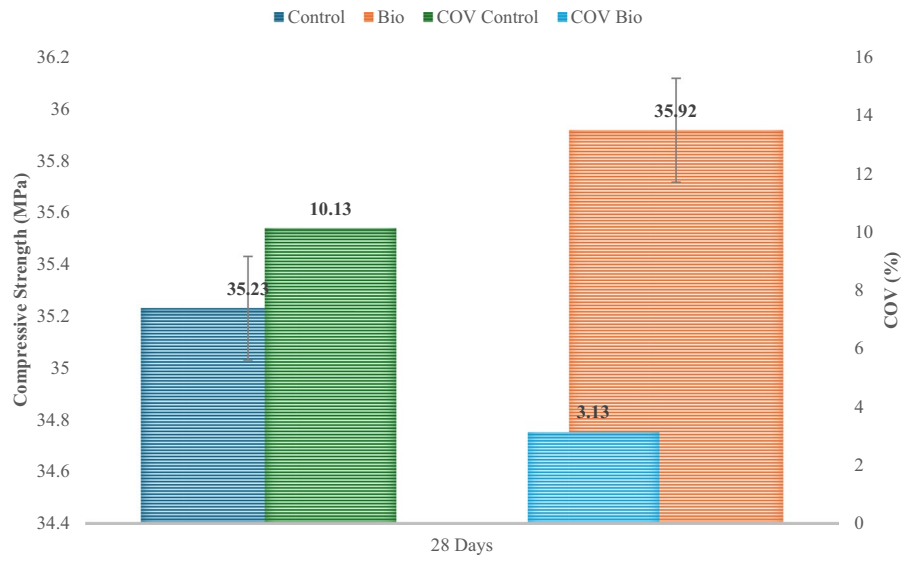

Fig. 2 Compressive strength of control and bio-modified specimens at 28-day ageing

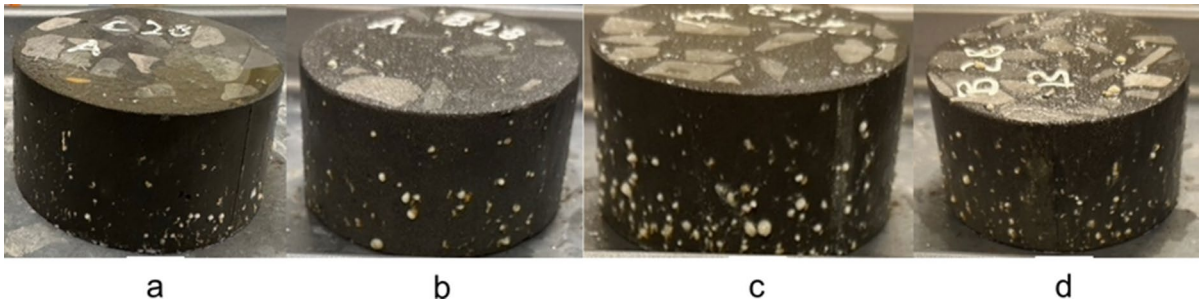

Fig. 3 Visual observation of geopolymer control and bio-modified specimens after acid exposure over days: **a** 3-(control), **b** 4-(bio), **c** 5-(control), **d** 10-(bio)

4.2 Surface observations and damage progression

Figure 3 illustrates the visual condition of control and bio-modified specimens following acid exposure. Both specimens exhibited white surface deposits, consistent with calcium ion leaching and gypsum formation under acid attack, as subsequently confirmed by EDS, XRF, and XRD analyses. No macrocracking or spalling was visually observed, consistent with the relatively low mass loss (Fig. 4) and retained mechanical integrity (Fig. 5) recorded over the 10-day exposure period. Surface deterioration was more prominent on the side faces, attributable to their greater exposed area and prolonged contact with the acidic solution.

When comparing these findings to previous studies, such as Wu et al. [35], they do not report macrocracks, and their findings align with the present research, suggesting that both acid and sulphate environments can lead to surface deterioration without visible cracks. This similarity is attributed to acid-induced ion exchange and microstructural weakening at the surface, which compromises the matrix without necessarily causing visible cracking.

4.3 Weight loss when exposed to acid

Figure 4a illustrates the mass loss of 100×50 mm geopolymer cylindrical specimens over a period of 10 days of acid exposure. All specimens exhibited measurable mass change after four days, primarily

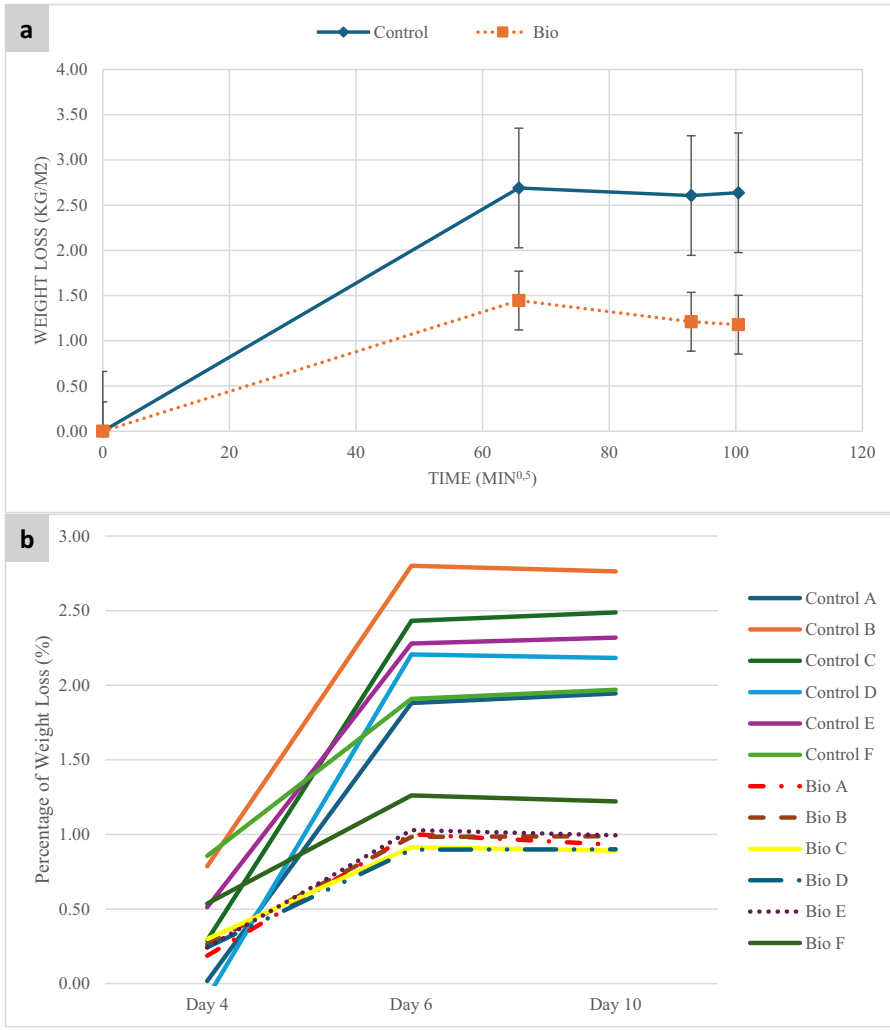

Fig. 4 **a** Weight loss (kg/m^2) of geopolymer control and bio-modified specimens during acid exposure, **b** percentage of weight loss for individual geopolymer specimens (each 100 × 50 mm cylinder) during acid exposure for control (A-F) and bio (A-F)

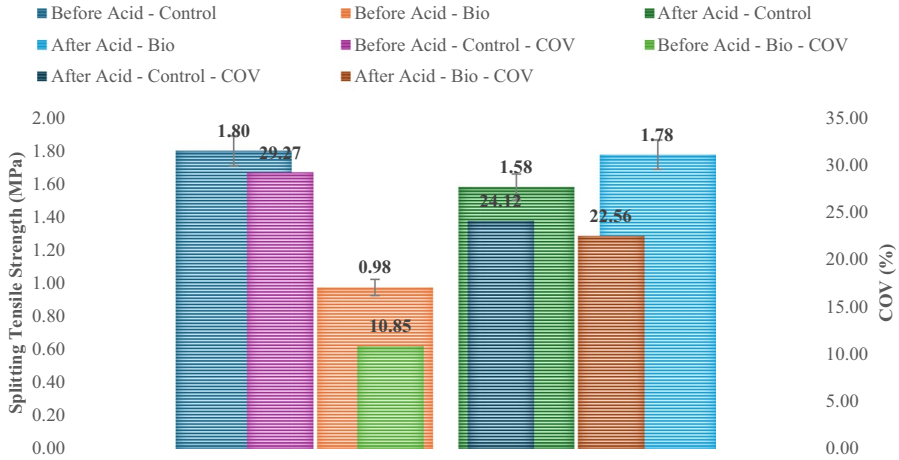

Fig. 5 Average splitting tensile strength (MPa) of control and bio-modified geopolymer specimens before and after 10-day exposure to 1% H_2SO_4

attributable to surface binder dissolution, which aligns with visual observations. However, bio-modified specimens showed markedly lower weight loss and greater stability compared to the control group. The increased mass variation observed in the control specimens may be partially due to the formation of gypsum ($CaSO_4 \cdot 2H_2O$) during acid interaction [47]. As depicted in Fig. 4b, the control specimens also demonstrated greater variability among individual specimens, whereas the bio-modified specimens exhibited more uniform performance, indicating enhanced resistance to acid-induced degradation.

The results from Zhao et al. [3] demonstrated that self-healing agents reduced mass loss and improved structural integrity under environmental stressors, a trend similarly observed in the present study, where bio-modified specimens exhibited lower and more consistent mass loss under acid exposure compared to controls. Similarly, Guo et al. [1] explored self-healing in fly ash-based engineered geopolymer composites, reporting that the incorporation of healing agents led to a recovery of mechanical properties after initial damage. Their findings suggested that healing agents effectively counteract the degradation caused by corrosive environments, resulting in less weight loss and improved durability. This supports the present research's conclusion that healing agents enhance the overall performance of geopolymer materials, particularly in harsh, acidic environments. In contrast, the control specimens in the present study displayed varying percentages of weight change and differing rates of change, indicating a less consistent performance. This variability suggests that without the influence of healing agents, the geopolymer specimens are more susceptible to degradation in acidic conditions. This observation is consistent with the findings of Rihan et al. [34], who noted that the mechanical properties of geopolymer concrete could significantly deteriorate under high alkaline concentrations, emphasising the importance of incorporating healing agents to maintain structural integrity.

4.4 Splitting tensile strengths

Figure 5 displays the splitting tensile strength of control and bio-modified geopolymer specimens prior to and following exposure to 1% H_2SO_4. The control specimens exhibited a decrease from 1.80 to 1.58 MPa, representing approximately a 13% reduction, indicative of deterioration stemming from acid attack. Conversely, the bio-modified specimens showed an increase from 0.98 to 1.78 MPa, an approximate 82% enhancement, implying ongoing bio-mediated reinforcement during exposure. This phenomenon is attributed to continuous biomineralisation processes, likely involving $CaCO_3$ precipitation, which enhance matrix densification and crack bridging, as corroborated by SEM–EDS observations detailed in Sect. 4.6 and Figs. 10, 11, 12, 13.

Additionally, it is noteworthy that chemical reactions predominantly occur in the surface regions; consequently, the top and bottom surfaces endure compressive stresses rather than tensile stresses during the splitting tensile strength tests. Wallah and Rangan [48] studied the effects of sulphuric acid on cylindrical specimens and found that only a 20 mm surface region was impacted by the acid attack, while the core regions maintained their integrity. This enhancement is attributed to ongoing hydration reactions and suggests that the core regions of the specimens remained unaffected by acid, as supported by Wallah and Rangan [48] findings on surface impact. Comparisons with studies by Zhao et al. [3] and Guo et al. [1] reveal that healing agents improve mechanical properties and durability under corrosive conditions, reinforcing the present research's conclusions.

4.5 Water absorption via capillary

Figure 6 illustrates the capillary water absorption characteristics of control and bio-modified specimens, with and without acid exposure. Both bio-modified and control specimens demonstrated comparable absorption rates during the initial phase. However, following acid exposure, bio-modified specimens consistently exhibited reduced total water uptake, as shown in Fig. 6a. This suggests a denser and less permeable pore structure, likely attributable to biomineralisation processes that diminish water ingress and increase resistance to acid attack. In specimens not subjected to acid exposure (Fig. 6b), the difference between control and bio-modified specimens was negligible, implying that bacterially mediated densification, through $CaCO_3$ precipitation and stable phase formation, is more pronounced under acidic conditions, where these processes are actively stimulated.

$CaCO_3$ precipitation occupies capillary pores, reducing effective pore radius and sorptivity. These

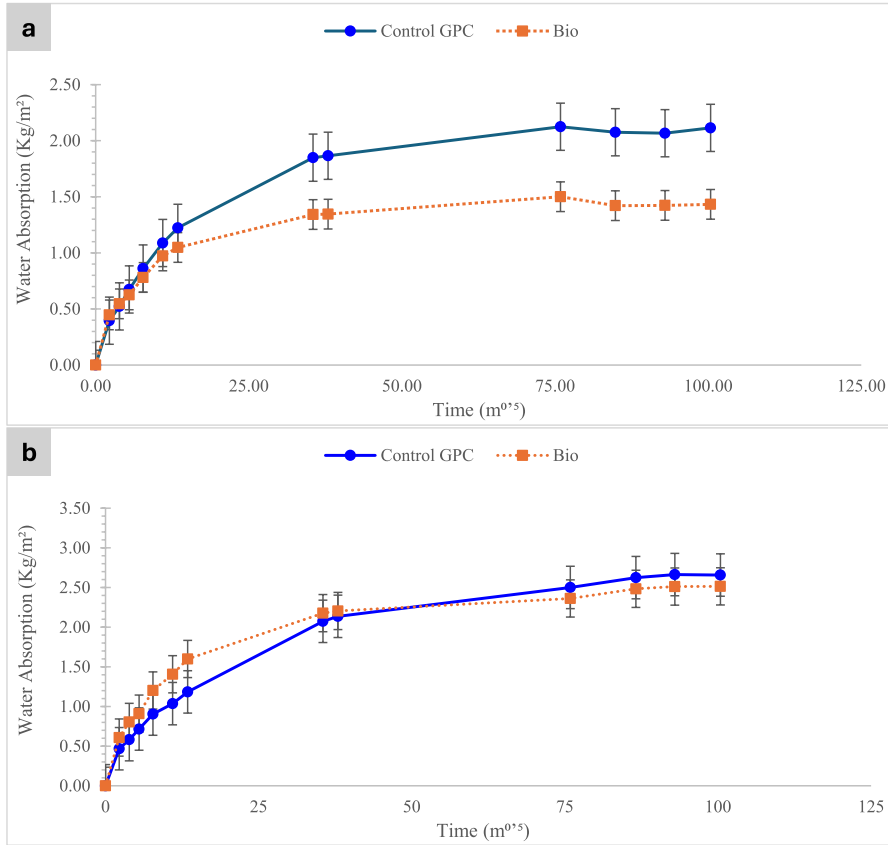

Fig. 6 Water absorption via capillary results for: **a** after acid exposure at 30 °C over 10 days, **b** without acid exposure at room temperature

results align with previous studies, such as those by Zhao et al. [3], which found that the incorporation of healing agents in geopolymer composites significantly enhanced their durability and reduced porosity, leading to lower water absorption rates. Zhao et al. [3] noted that self-healing agents can fill microcracks and voids, thereby improving the material's impermeability. Similarly, Guo et al. [1] reported that self-healing agents in fly ash-based geopolymer composites contributed to a denser microstructure, resulting in decreased water absorption and enhanced performance in aggressive environments. In contrast, the findings of Makilan et al. [49] indicated that while healing agents improved mechanical properties, their effect on water absorption was less pronounced. This suggests that the efficacy of bio-based healing agents may vary with formulation and exposure conditions. The present research supports this, as the *Shewanella oneidensis* bioproduct had a negligible impact on water absorption without acid exposure, indicating that acidic conditions are necessary to stimulate the bacterial activity driving matrix densification.

4.6 SEM–EDS analysis

4.6.1 Effect of bacteria on the geopolymer before acid immersion

SEM images before acid exposure (Fig. 7a, b) reveal that the control samples possess a more porous microstructure with discernible microcracks, especially within the interfacial transition zone (ITZ). Conversely, the bio-modified specimens exhibit a denser and more homogeneous matrix with fewer microvoids, indicative of microstructural refinement resulting from bacterial integration. EDS spectra (Fig. 7c–d) display low calcium levels but detectable carbon and oxygen, implying early carbonate-phase formation. These findings suggest that bacterial incorporation enhances matrix densification and pore obstruction before acid exposure, thereby likely contributing to increased durability observed subsequently, in alignment with prior research on bio-modified geopolymer systems [50–53].

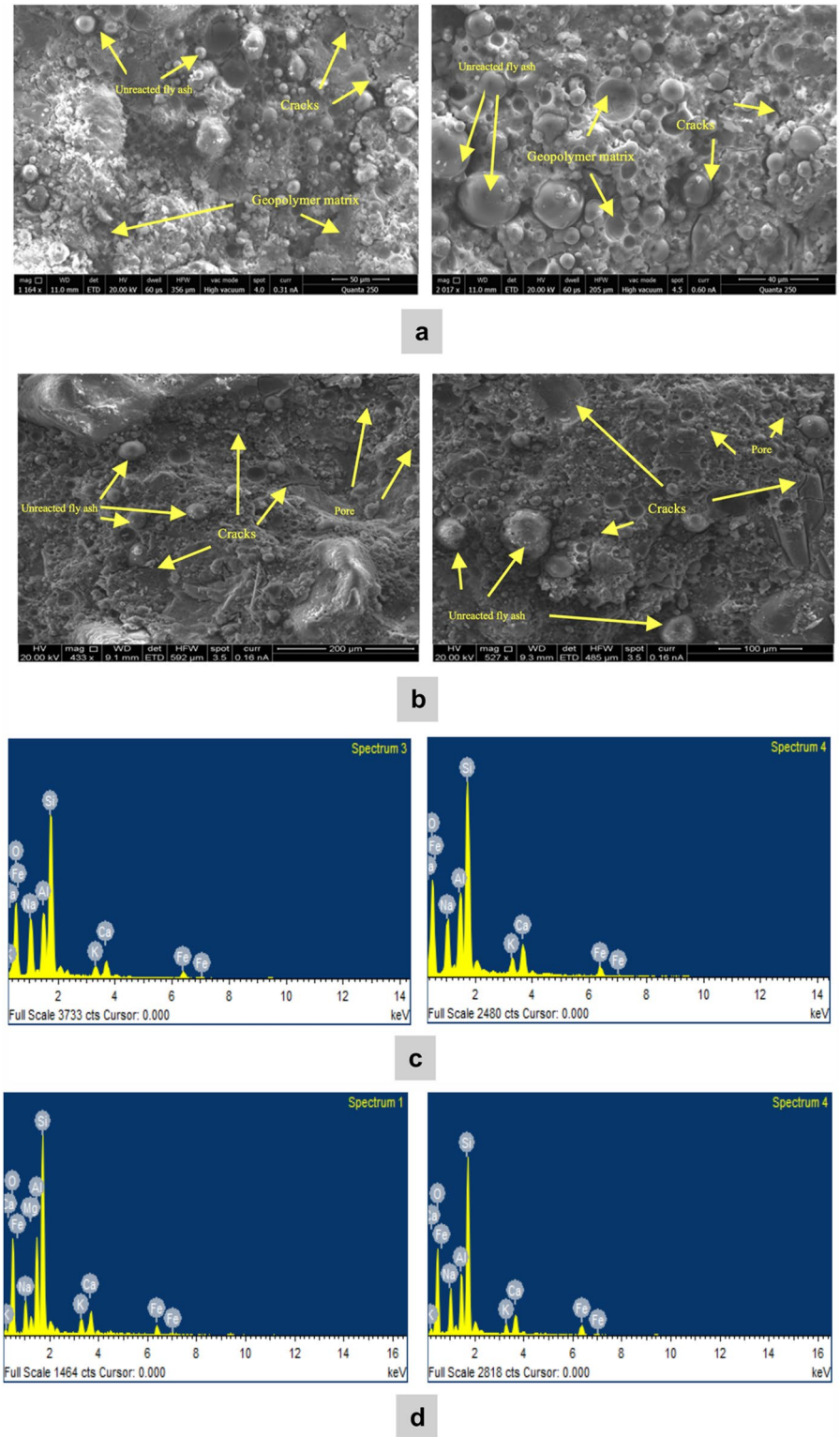

Fig. 7 SEM images before acid immersion for: **a** control samples, **b** bio-modified samples, EDS spectra before acid immersion for: **c** control samples, **d** bio-modified samples

Table 2 EDS analysis for control and bio-modified samples before acid immersion

	Element	Weight %	Atomic %		Element	Weight %	Atomic %
Control	O	45.36	59.67	Bio	O	52.91	66.84
	Na	11.15	10.22		Na	8.32	7.33
	Al	9.16	7.16		Al	8.20	6.16
	Si	24.28	18.21		Si	21.09	15.21
	K	2.26	1.22		K	2.01	1.05
	Ca	3.62	1.90		Ca	3.51	1.78
	Fe	3.26	1.23		Fe	3.53	1.28

Table 3 Chemical compositions of bio-modified and control samples before acid immersion (wt.%)

Chemical Compositions	SiO_2	Al_2O_3	Fe_2O_3	P_2O_5	SO_3	TiO_2	CaO	K_2O	MgO	Na	Cl
Bio	41.7	11	3.5	0.152	0.609	0.518	6.69	1.59	0.925	8.12	0.012
Control	42.7	11.3	3.56	0.144	0.641	0.51	6.24	1.67	0.87	7.54	0.0088

Table 2 presents the elemental composition of control and bio-modified specimens prior to acid exposure. The bio-modified samples exhibit slightly lower Ca and Na but higher O and C contents, indicating the presence of early carbonate-related phases that may influence the denser microstructure observed in SEM images. Additionally, the marginally higher Fe content in the bio-modified specimens could facilitate the formation of iron-bearing phases such as andradite, as later confirmed by XRD analysis (Fig. 13). Overall, these findings suggest that bacterial incorporation enhances early matrix stabilisation prior to acid exposure.

The chemical composition of the bio-modified and control specimens before acid exposure was determined using XRF, as presented in Table 3. It demonstrates comparable SiO_2 and Al_2O_3 contents in both control and bio-modified samples, suggesting analogous geopolymer structures. The bio-modified specimens show a marginally higher CaO content (6.69%), potentially attributed to interactions with the bacterial medium that may facilitate early gel formation. Overall, the consistent Si-Al composition establishes a stable baseline for assessing chemical modifications following acid exposure.

4.6.2 *Effect of acid immersion on the geopolymer microstructure*

SEM images following acid immersion (Fig. 8a, b) demonstrate more pronounced surface deterioration in the control samples, including microcrack development, weakening of the ITZ, and partial dissolution of the binder. EDS spectra (Fig. 8c) reveal decreased intensities of Si and Al, indicative of leaching from the geopolymeric phases. Conversely, the bio-modified specimens display a denser residual matrix and reduced surface erosion under comparable exposure conditions. EDS data (Fig. 8d) suggest some ion redistribution, with diminished Ca and slightly elevated Fe signals, implying acid-induced leaching and potential suppression of bacterial activity at low pH. However, XRD and FTIR analyses confirm the continued presence of andradite and a reduction in silicate depolymerisation, indicating that bacterial incorporation enhances phase stability and resistance to acid-related degradation.

Table 4 delineates the elemental composition of both control and bio-modified specimens following acid immersion. The bio-modified samples exhibited higher concentrations of calcium and iron relative to the control specimens, indicative of diminished decalcification and enhanced phase stability under acidic conditions. The increased oxygen levels and maintained calcium content imply the presence of carbonate-related phases, corroborating FTIR and XRD analyses. These results suggest that bio-modification confers improved resistance to acid-induced leaching and contributes to the stabilisation of the geopolymer matrix.

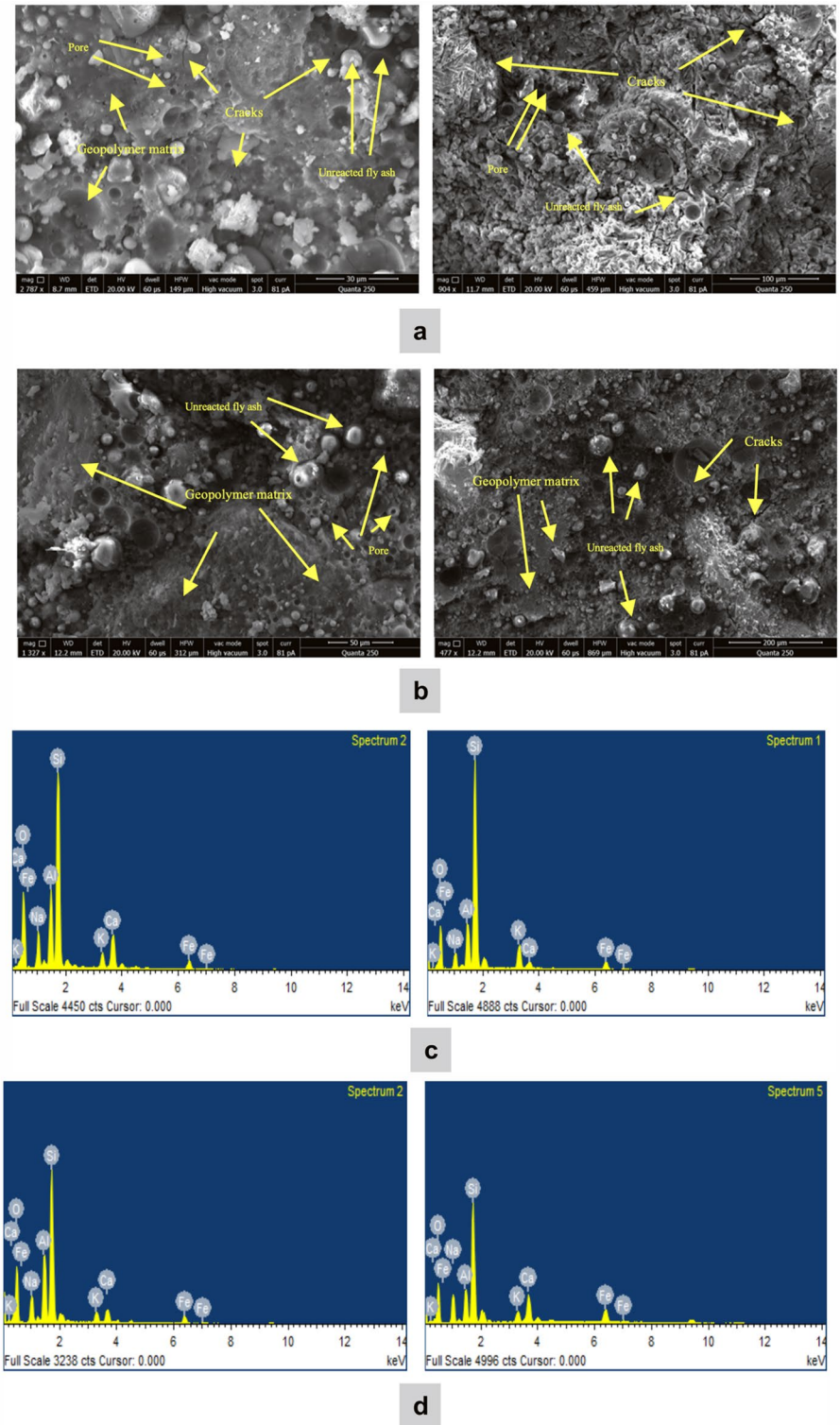

Fig. 8 SEM images after acid immersion for: **a** control samples, **b** bio-modified samples, EDS spectra for **c** control samples, **d** bio-modified samples, after acid immersion

Table 4 EDS analysis for control and bio-modified samples after acid immersion

	Element	Weight %	Atomic %		Element	Weight %	Atomic %
Control	O	43.65	65.48	Bio	O	48.85	65.16
	Na	5.77	5.00		Na	7.52	6.98
	Al	6.09	5.42		Al	6.53	5.11
	Si	22.47	18.95		Si	20.24	15.34
	K	2.57	2.06		K	1.87	1.01
	Ca	2.72	1.74		Ca	3.73	1.97
	Fe	3.70	1.37		Fe	5.75	2.17

Table 5 Chemical compositions of bio-modified and control Samples after acid immersion (wt.%)

Chemical Compositions	SiO_2	Al_2O_3	Fe_2O_3	P_2O_5	SO_3	TiO_2	CaO	K2O	MgO	Na	Cl
Bio	45.7	11.9	4.35	0.2	0.42	0.556	5.33	1.82	0.932	6.46	0.167
Control	46.8	12.9	4.47	0.202	0.418	0.591	7.69	1.92	1.08	7.54	0.0205

The chemical composition of the bio-modified and control samples after acid immersion was determined using XRF, as presented in Table 5.

Post-acid immersion, both control and bio-modified samples showed increased SiO_2 and Al_2O_3 (Table 5), likely from leaching of soluble phases like Ca, Na, and K. CaO in bio-modified samples dropped over 20%, indicating decalcification. The bio-modified samples retained more Na and Mg than controls, possibly due to microstructural differences from the healing agent. XRF and SEM–EDS (Tables 3, 4, 5, Figs. 7, 8, 9, 10) analyses both indicated structural degradation and increased porosity from leaching effects in control samples. SEM analysis at 180 days (Fig. 9) supports the presence and potential survival of bacterial influence post-curing in the geopolymer matrix.

In the bio-modified samples (Fig. 9b), spherical inclusions and mineral nodules were observed, features commonly associated with microbial precipitation and metabolic by-products. After acid exposure (Fig. 9c), these features persisted, with retained mineralisation and denser microstructural regions, suggesting either partial survival of bacterial residues or their stabilising effect on the matrix. In contrast, the control sample (Fig. 9a) exhibited irregular morphology with no evidence of bacterial activity or biomineralisation.

The high-magnification SEM–EDS mapping (Figs. 10a–c) provides further evidence of the microstructural and chemical differences between control and bio-modified samples. In the control specimen (Table 6), elements such as Al and Si were unevenly distributed across the cracked matrix, with Fe levels remaining negligible (< 1 at.%), indicating no bacterial influence. Elemental maps for K, Mg, and Ti, which were not directly implicated in the degradation mechanism, are

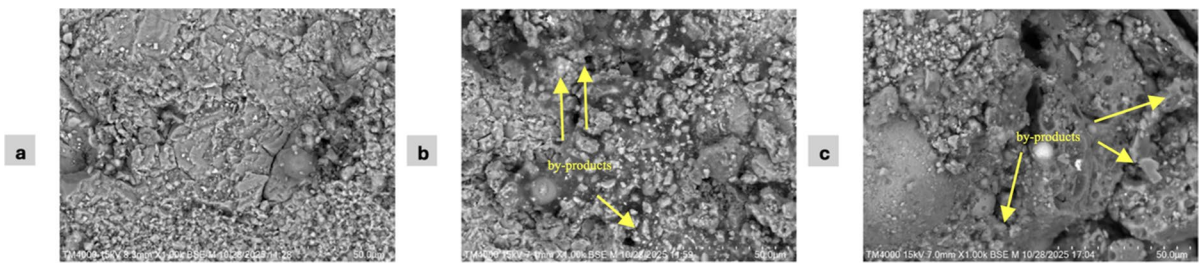

Fig. 9 SEM micrographs at 180 days of geopolymer specimens: **a** Control sample before acid exposure, **b** bio-modified sample before acid exposure, **c** bio-modified sample after 10-day acid immersion

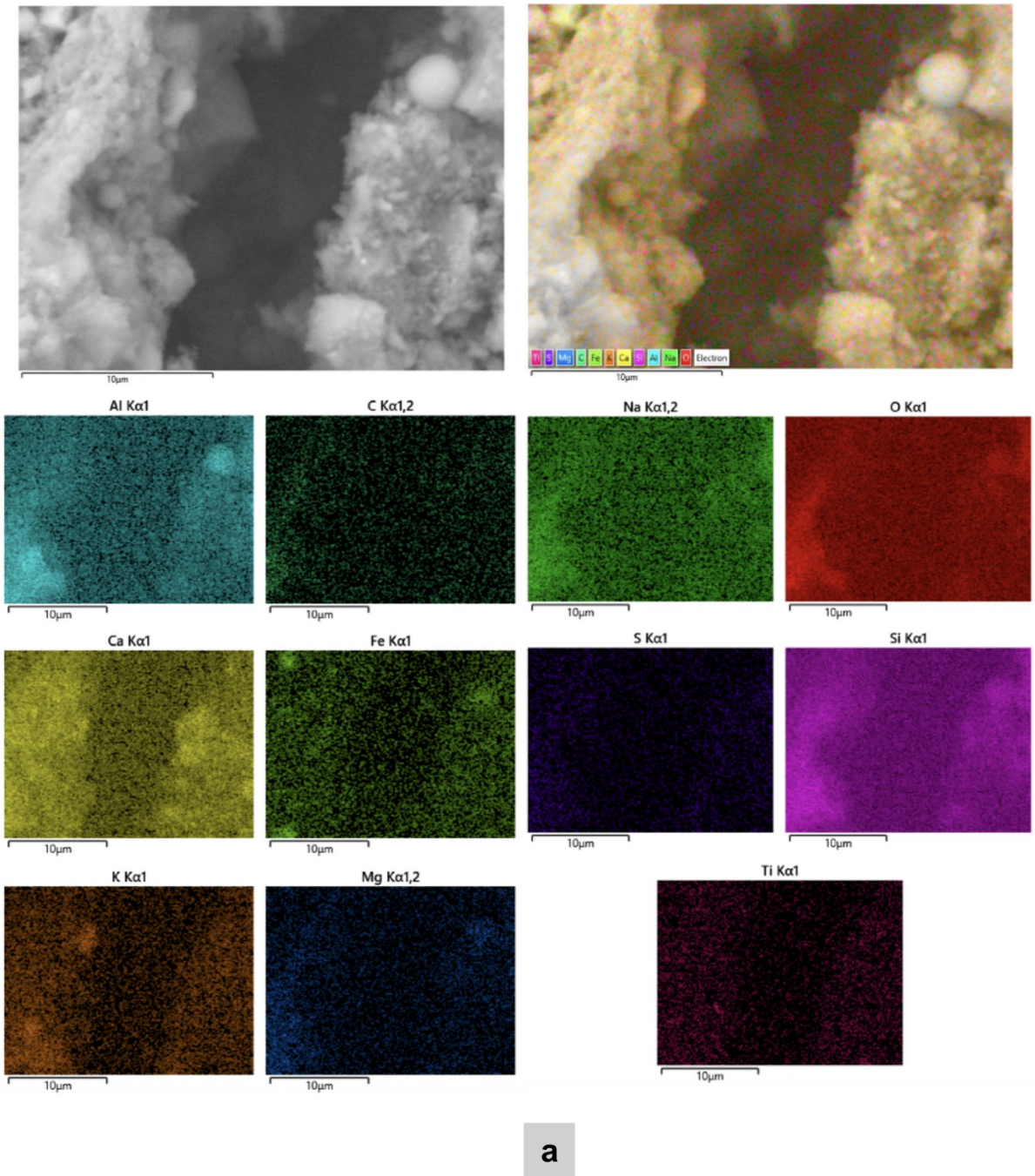

Fig. 10 SEM–EDS elemental maps of geopolymer samples (at 180 days) showing microbial influence in: **a** bio-modified sample without acid exposure, **b** control sample without acid exposure, **c** bio-modified sample with 10-day acid exposure

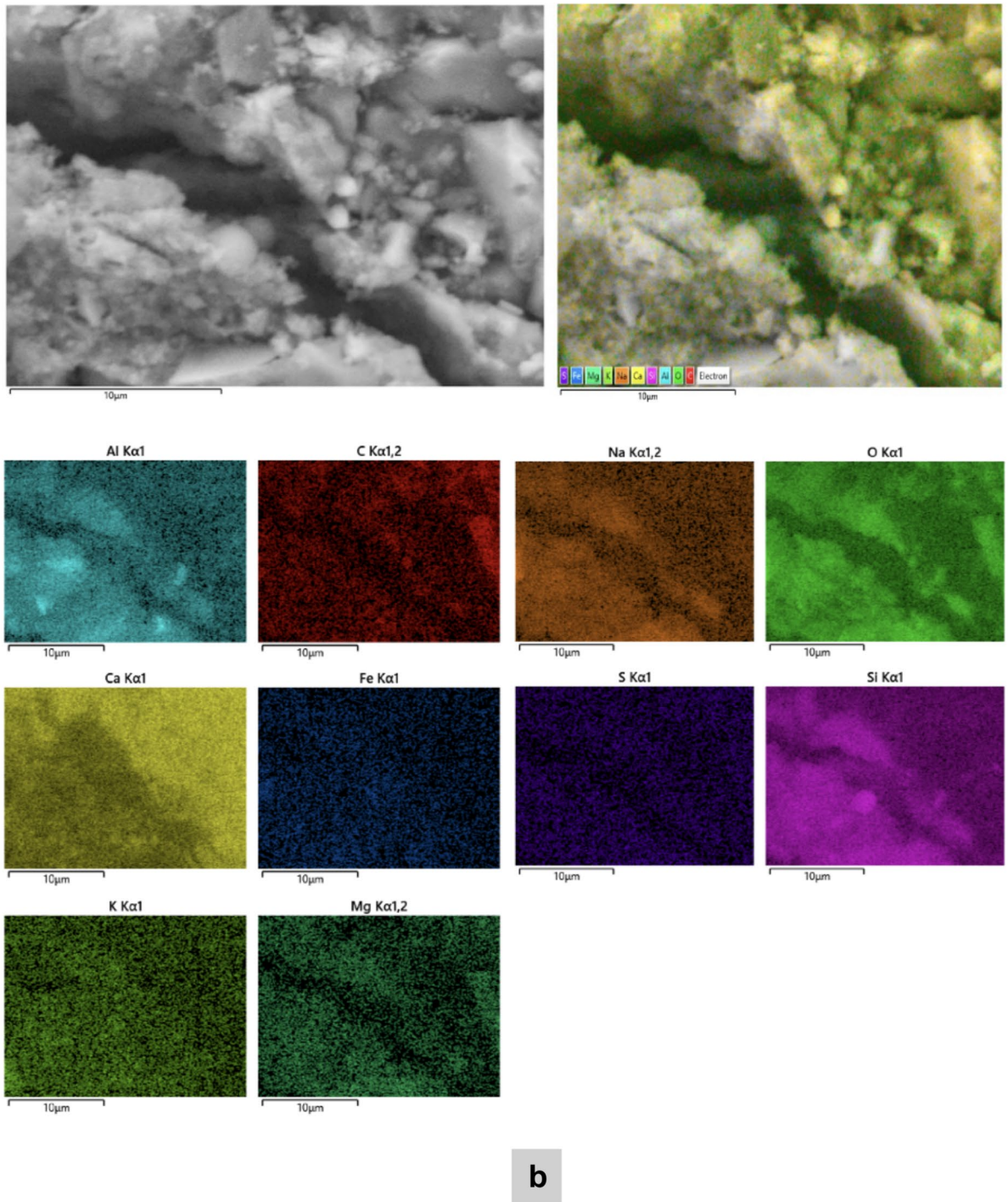

Fig. 10 (continued)

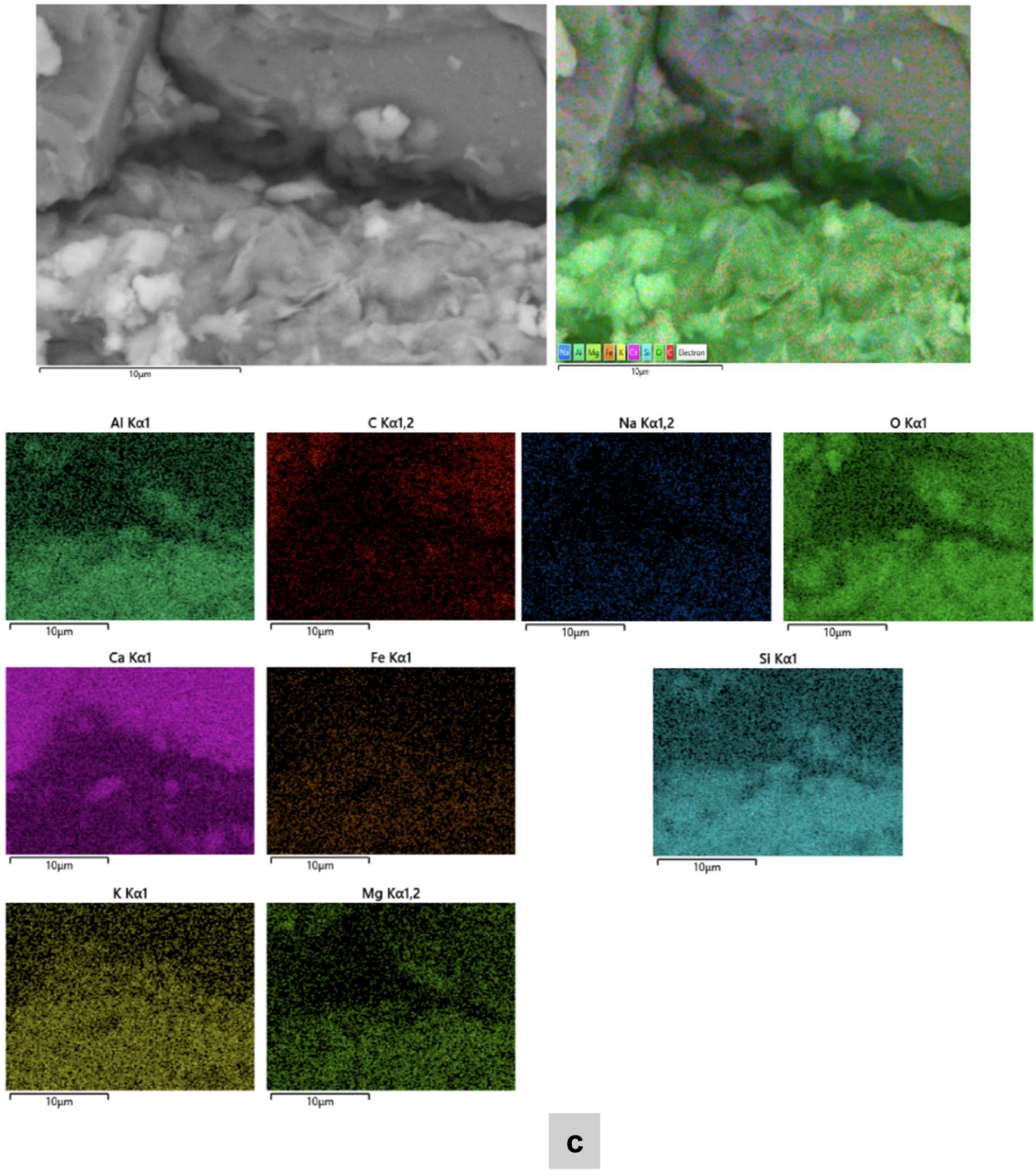

Fig. 10 (continued)

Table 6 EDS analysis of control samples without acid immersion and bio-modified samples with and without acid exposure—at 180 days (wt.%)

Element	O	C	Si	Ca	Na	Al	Fe	K	Mg	Ti	S
Bio—before acid exposure	57.93	15.90	11.72	5.12	3.61	3.14	1.26	0.79	0.32	0.13	0.08
Bio—after acid exposure	58.93	19.22	5.78	9.80	0.44	1.24	0.86	1.24	0.90	-	-
Control—before acid exposure	60.48	17.84	9.93	5.53	2.96	2.07	0.40	0.35	0.32	0.07	0.06

provided (where present) in Appendix A for completeness. Conversely, the bio-modified sample before acid exposure (Fig. 10a) demonstrated a more uniform spatial distribution of Al, Si, and Na, implying improved matrix homogeneity due to bio-modification. Additionally, the increased Fe content in bio-modified samples supports the role of *Shewanella* species in bio-mediated Fe metabolism, given its known iron-reduction capabilities [54]. Post acid exposure (Fig. 10c), the bio-modified sample maintained key mineral phases, with Fe and Ca still detectable within the matrix. This observation corroborates the hypothesis that bacterial activity promotes both early densification and enhanced chemical stability under acidic conditions (Fig. 11).

4.6.3 Leaching

Leaching is a phenomenon characterised by the dissolution and migration of ions from the geopolymer matrix upon exposure to aggressive environments. In samples immersed in acidic conditions, leaching is frequently associated with the following effects:

- The loss of calcium and alkali elements (Na, K, and Ca) is attributed to acid dissolution (Fig. 12, steps 1–2).
- The degradation of the geopolymer network, specifically the Si–O-Al bonds, resulting from proton exchange.
- The formation of secondary degradation products, which may either precipitate or remain in a dissolved state [55, 56].
- The following figure (Fig. 12) is a schematic representation comparing ionic leaching pathways in control vs bio-modified specimens under H_2SO_4 attack.

The white surface deposits seen in Fig. 11a, along with visible deterioration, qualitatively indicate the leaching of calcium- and alkali-bearing phases (Fig. 12, step 3), as further corroborated by EDS and XRD, despite the lack of quantitative leachate ion analysis.

4.6.4 SEM–EDS assessment of the leached material

SEM analysis of the leached powder, shown in Fig. 11b, revealed a porous, flaky morphology characterised by fine, fragmented particles. EDS analysis, presented in Fig. 11c, of these leached deposits confirmed their composition as predominantly:

- Elevated oxygen content, suggestive of oxidation or hydration processes.
- Presence of Si and Al, indicating possible partial dissolution of the geopolymer matrix.
- Notable depletion of Na, K, and Ca, aligning with the process of ion leaching pathway illustrated in Fig. 12.
- Traces of phosphorus (P) and S, which may result from environmental contamination or byproducts produced by acid-induced reactions.

Significantly, the observed decrease in the Si/Al ratios in the leached material implies ongoing geopolymer dissolution, potentially leading to a weakening of the structural matrix.

The elemental composition of the leached powder (see Table 7) demonstrates extensive matrix degradation following acid exposure, characterised by elevated O levels and reduced Ca content, indicative of significant decalcification. Increased Si and Na concentrations suggest selective leaching of soluble phases and the development of a residual silica-rich framework. The detection of sulphur supports

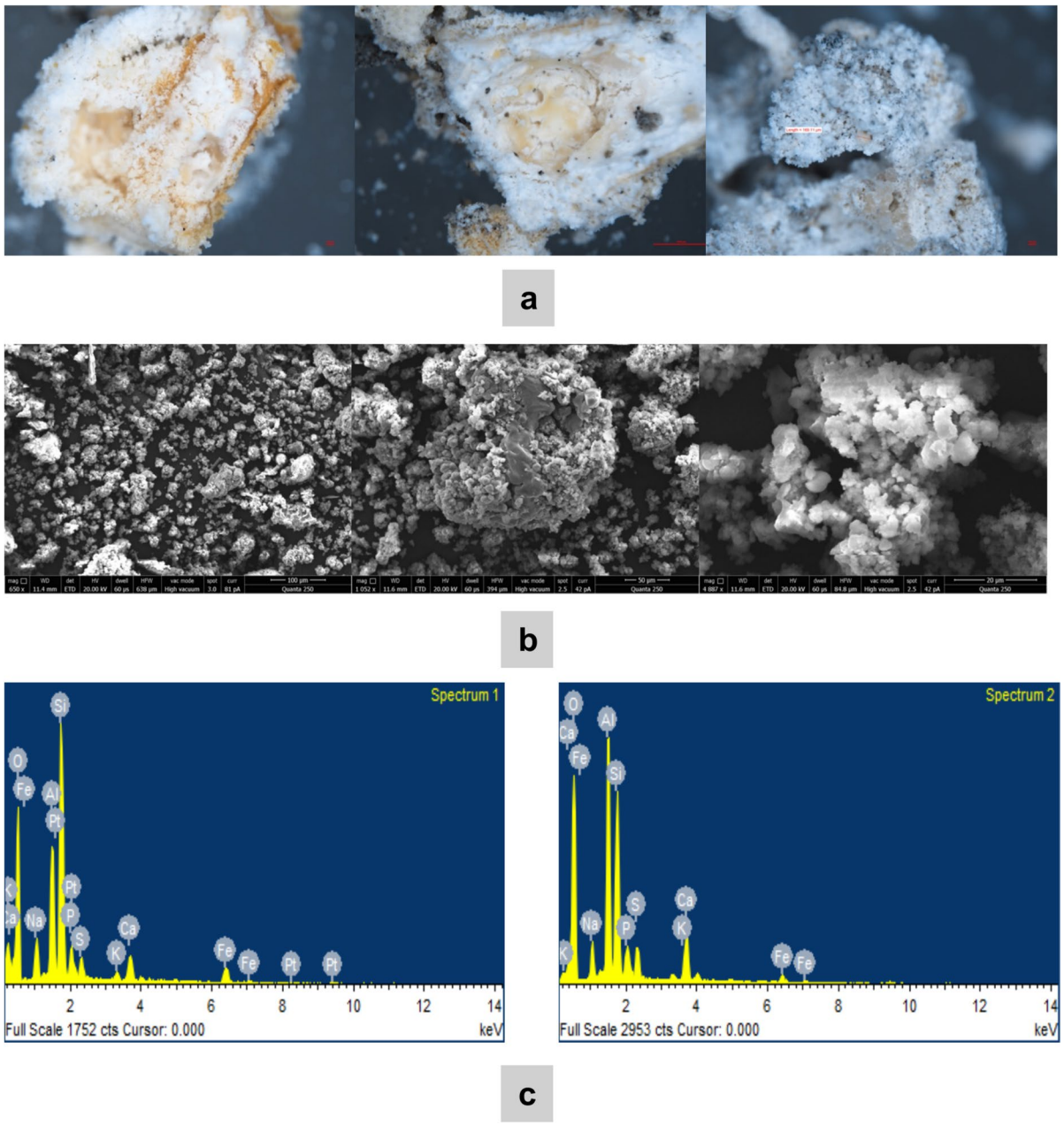

Fig. 11 **a** Microscope images of surface white powder deposits formed after 10-day immersion in 1% H_2SO_4, **b** SEM images of the leaching powder after acid immersion, **c** EDS for leaching powder after acid Immersion

gypsum formation during the acid attack, while trace Fe implies partial preservation of iron-bearing phases such as andradite, consistent with XRD analysis. When compared to the bulk compositions outlined in Tables 2 and 4, these findings imply that bio-modified samples more effectively retained Ca and maintained structural integrity under acidic conditions.

Based on the elemental compositions derived from EDS results, the molar ratios of Si/Al, Na/Al, Ca/Al, and Fe/Al were rigorously evaluated for the leached powder, control, and bio-modified samples,

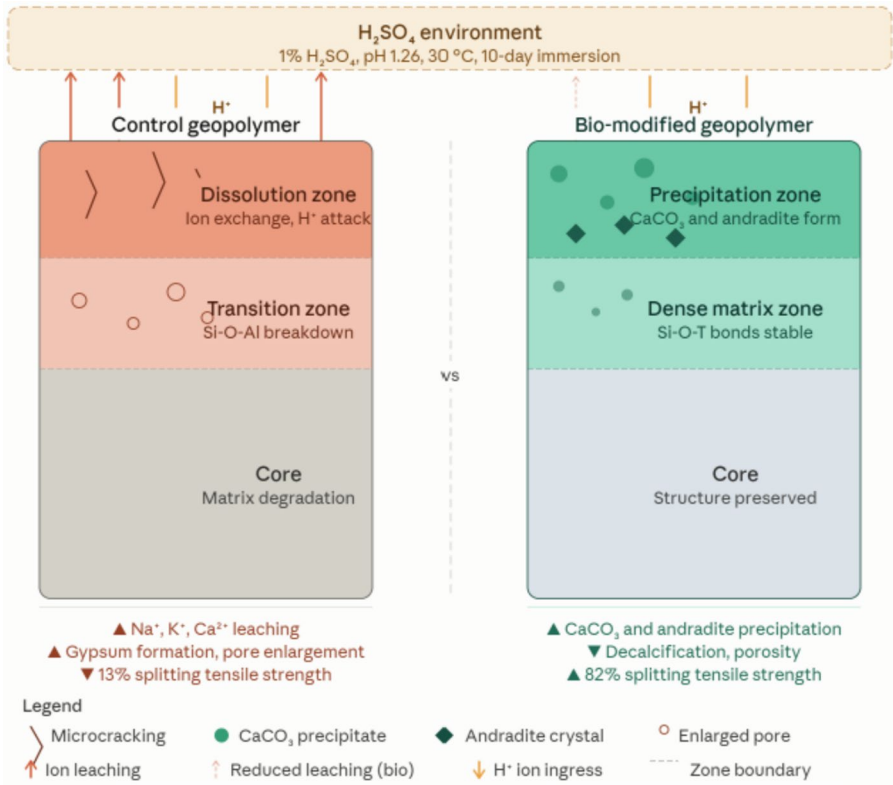

Fig. 12 Schematic representation comparing ionic leaching pathways in control vs bio-modified specimens under H_2SO_4 attack

Table 7 EDS analysis for leaching powder after acid immersion

	Element	Weight %	Atomic %
Leaching Powder	O	61.92	74.61
	Na	4.11	3.45
	Al	12.05	8.59
	Si	12.87	8.85
	S	1.95	1.18
	K	0.56	0.28
	Ca	3.35	1.61
	Fe	2.02	0.70

both prior to and following acid immersion. These molar ratios yield essential insights into the degree of geopolymerisation and the inherent acid resistance characteristics of geopolymer matrices.

- *Leached powder*
  - Si/Al = 1.07
  - Na/Al = 0.34
  - Ca/Al = 0.28
  - Fe/Al = 0.17

The leached powder showed a low Si/Al ratio (1.07) and a depleted Na/Al ratio (0.34), suggesting significant alkali loss and structural collapse of the aluminosilicate matrix due to acid attack. In control specimens, Si/Al ratios increased from 2.65 to 3.69 after acid exposure, indicative of aluminium leaching and progressive degradation of the matrix. Conversely, bio-modified samples exhibited smaller variations in Si/Al ratios (2.57–3.10) and higher Ca/Al and Fe/Al ratios post-exposure, demonstrating enhanced retention of calcium and iron phases. According to the literature [57–59], Optimal mechanical performance usually occurs at Si/Al ratios of 1.5–2.5. Although both control and bio-modified samples exceed this range after acid treatment, the higher Si/Al ratio in bio-modified specimens indicates better stability, likely due to biological processes reducing Al leaching. The elevated Fe/Al ratio corroborates the formation or preservation of stable phases such as andradite, as confirmed by XRD analysis. These

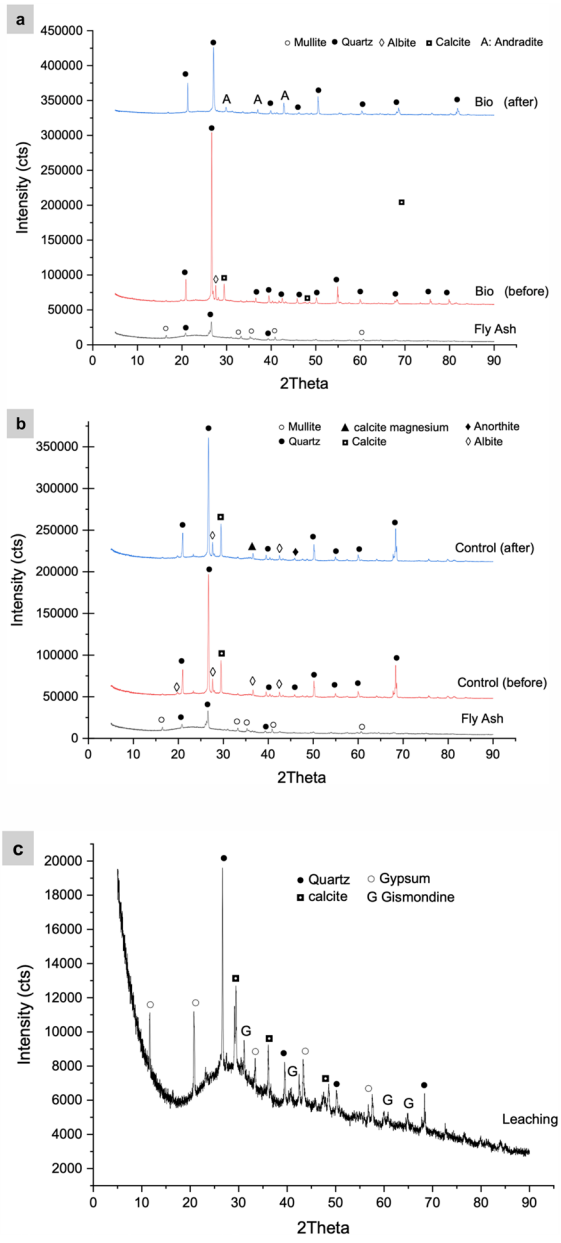

Fig. 13 XRD patterns of: **a** fly ash, bio-modified samples before and after acid immersion, highlighting the evolution of crystalline phases, **b** fly ash, control samples before and after acid immersion, showing changes in peak intensities and formation of degradation-associated minerals, **c** leached powder (L) deposits formed after 10-day acid immersion

molar ratios suggest that bio-modification enhances resistance to acid-induced leaching by stabilising the aluminosilicate network and maintaining key structural components.

- *Control (before/after acid)*
  - Si/Al = 2.65/3.69
  - Na/Al = 1.22/0.95
  - Ca/Al = 0.40/0.45
  - Fe/Al = 0.36/0.61
- *Bio-modified specimen (before/after Acid)*
  - Si/Al = 2.57/3.10
  - Na/Al = 1.01/1.15
  - Ca/Al = 0.43/0.57
  - Fe/Al = 0.43/0.88

The process of acid immersion markedly accelerated leaching through several mechanisms:

– Hydrogen ion exchange (H^+ attack):

Acidic H^+ ions replace Na^+, K^+, and Ca^{2+} in the geopolymer, disrupting the Si–O-Al network. Bio-modified samples showed reduced Si and Al loss (EDS) and more stable Si–O–T bonds (FTIR), confirming better preservation of the aluminosilicate framework. XRD results further support this with clearer quartz retention and Andradite formation, indicating a more intact matrix structure in Bio

– Decalcification:

The low calcium content observed in EDS results indicates the dissolution of minor calcium-rich phases, compromising the structural integrity of the geopolymer.

Leaching under acidic conditions poses significant challenges, particularly for geopolymers with high alkali content, as the presence of alkalis facilitates rapid dissolution in aggressive environments.

4.7 X-ray diffractometer

X-ray diffraction (XRD) analysis was conducted to characterise the crystalline phases in raw FA and the control and bio-modified specimens prior to and following immersion in sulphuric acid, as well as the leached powder obtained post-immersion. The resulting patterns are illustrated in Fig. 13.

Figure 13 displays the XRD patterns of fly ash, control, and bio-modified geopolymer samples before and after acid immersion. The dominant crystalline phases originating from the raw fly ash are quartz and mullite, while the broad amorphous hump between 20–35° 2θ indicates the presence of geopolymeric aluminosilicate gel. Following acid immersion, the control samples exhibit a decrease in calcite peak intensity and an increase in quartz crystallinity, reflecting decalcification and dissolution of calcium-bearing binding phases. Conversely, the bio-modified samples demonstrate enhanced structural stability, as evidenced by the retention of albite and anorthite reflections and the formation of iron-bearing andradite (approximately at 32° 2θ), which correlates with improved resistance of Fe-Ca silicate phases under acidic conditions. This behaviour is also consistent with findings by El Alouani et al. and Grengg et al. [50, 51]. This interpretation aligns with SEM–EDS observations showing higher Fe retention in bio-modified specimens and suggests that bio-modification enhances resistance to acid-induced matrix degradation. The XRD pattern of the leached powder is predominantly composed of quartz, with residual calcite and gypsum-related phases, confirming the dissolution of calcium-bearing components and the formation of secondary sulphates during acid attack.

A comparison of the results of the present study with previous studies shows that geopolymer concretes, due to their chemical composition and more resistant structure, perform better in corrosive conditions such as sulphuric acid. For example, Guo et al. [1] reported that fly ash with SiO_2 content higher than 60 wt.% can positively impact the quality of geopolymer concrete. In contrast, the present study indicates that fly ash with 56.3 wt.% SiO_2 is still recognised as a suitable material for producing geopolymers, demonstrating the impact of fly ash quality on the final performance of the geopolymer. In another study, Zhao et al. [3] examined the effects of CaO on self-healing products in geopolymers and showed that CaO at low levels positively affects mechanical properties and self-healing. However, in the present study, the reduction of CaO after immersion in acid indicates the vulnerability of geopolymer concretes in corrosive conditions. Khan et al. [2] also showed a significant reduction in calcite peaks in OPC samples after immersion in sulphuric acid, which aligns with the findings of the present study and indicates that both types of concrete (OPC and geopolymer) are sensitive to acidic compounds.

4.8 FTIR analysis

FTIR spectra (Fig. 14) were employed to assess chemical modifications in the geopolymer matrix prior to and following acid exposure. The raw fly ash exhibits a prominent Si–O–T (T=Si or Al) vibration band near approximately 1020 cm^{-1}, indicative of the amorphous aluminosilicate structure. Post-geopolymerization, this band shifts to approximately 980–985 cm^{-1} in both control and bio-modified samples, signifying the development of the geopolymeric gel network. Upon acid exposure, the Si–O–T band shifts to higher wavenumbers (~990–995 cm^{-1}) and exhibits a reduction in intensity, reflecting depolymerisation and dealumination of the aluminosilicate framework, with more pronounced effects observed in the control specimens. Elevated bands around 1410 cm^{-1} and 1640 cm^{-1} denote increased carbonation and water adsorption associated with acid-induced leaching processes. The spectrum of the leached powder displays a prominent carbonate band and a diminished Si–O–T signal, confirming the dissolution of the geopolymer matrix and subsequent reprecipitation of $CaCO_3$. No bands related to ettringite were identified, corroborating the findings from XRD analysis.

The FTIR peak assignments outlined in Table 8 indicate that acid exposure leads to partial depolymerisation of the geopolymer network by proton-induced disruption of Si–O-Al bonds and leaching of alkali and calcium ions. Conversely, the bio-modified samples demonstrate relatively enhanced structural stability under acidic conditions [60, 61].

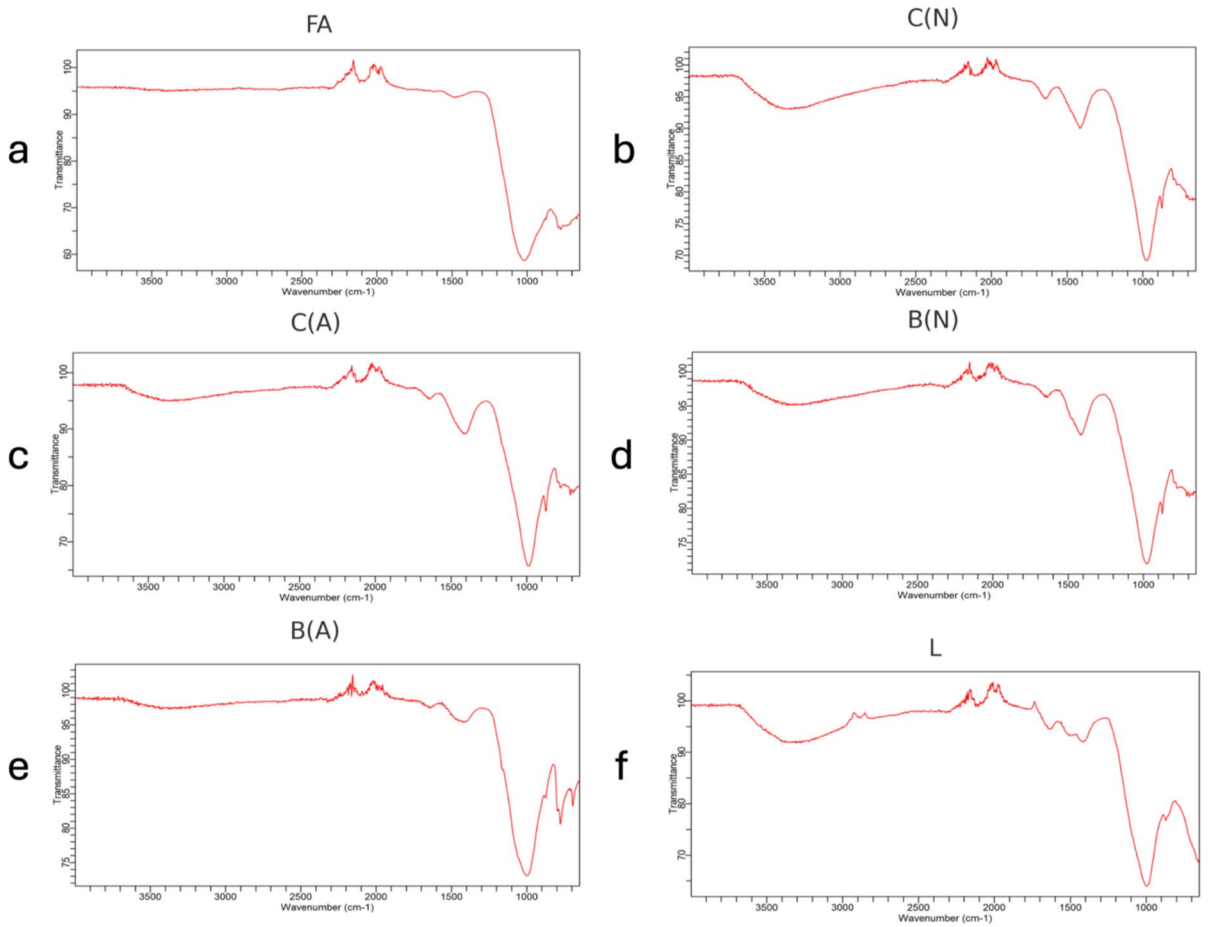

Fig. 14 FTIR spectra for **a** FA—Fly Ash, **b** B(N)—Bio-modified before acid, **c** C(N)—Control before acid, **d** B(A)—Bio-modified after acid, **e** C(A)—Control after acid, **f**) L—Leached powder

Table 8 FTIR peak assignments and their interpretation in geopolymer samples

Wavenumber (cm^{-1})		Assignment	Interpretation
~1020 (FA)	Si–O–T asymmetric stretching (T=Si or Al)		Indicative of amorphous aluminosilicate in raw fly ash
~980–985 (C(N), B(N))	Shifted Si–O–T band		Formation of geopolymeric gel (polycondensation of aluminosilicate species)
~990–995 (C(A), B(A))	Slight shift of Si–O–T post-immersion		Partial depolymerisation and dealumination under acid attack
~1410–1420	CO_3^{2-} asymmetric stretching		Carbonation of surface layers; increases post-acid exposure and in leached powder
~1640	H–O–H bending vibration		Presence of bound or adsorbed water in the matrix
~3400	O–H stretching		Hydroxyl groups; indicates water absorption and possible structural damage

4.9 Chemical mechanisms behind material degradation

The findings from EDS, XRD, and FTIR analyses collectively demonstrate that acid exposure has disrupted the geopolymer framework through three interconnected mechanisms.

First, the leaching of alkali and alkaline earth metals (sodium, potassium, calcium), evidenced by reduced Na, K, and Ca in EDS (Table 4) and decreased calcite peak intensity in XRD (Fig. 13b), exacerbates the weakening of structural bonds. Bio-modified specimens showed greater retention of these elements, consistent with the preserved albite and anorthite reflections observed in XRD (Fig. 13a).

Second, a decrease in aluminium coordination, reflected in the progressive Si/Al ratio increase in EDS molar ratio analysis and the shift of the Si–O–T band to higher wavenumbers in FTIR (Fig. 14), results in diminished strength of the geopolymer backbone. The less pronounced Si–O–T band shift in bio-modified specimens confirms reduced dealumination, as discussed in Sect. 4.8.

Third, the development of silica gel, which may either solidify or erode over time leaving behind a porous structure, is supported by the broad amorphous hump in XRD patterns and the reduced Si–O–T signal intensity in FTIR spectra of control specimens' post-exposure.

According to existing literature [45, 62–65], sustained acid exposure on geopolymers induces a three-stage degradation process:

1. Ion exchange stage: Initial leaching of sodium, potassium, and calcium.
2. Si/Al network breakdown: Formation of gel and increased porosity.
3. Complete matrix disintegration: Severe reduction in mechanical strength and integrity.

While SEM–EDS, XRD, and FTIR collectively confirm geopolymer susceptibility to acid degradation in acidic wastewater, bio-enhanced geopolymer concrete demonstrates significant potential for improved durability, as evidenced by the retained crystalline phases (Sect. 4.7) and stable Si–O–T bonds (Sect. 4.8) observed in bio-modified specimens. The simplified chemical formulae presented in Eqs. 1–5 consolidate the key acid-induced reactions identified across Sects. 4.6.3–4.9. Equation 1 shows the initial dissociation of H_2SO_4 into H^+ and SO_4^{2-} ions. Equation 2 depicts the ion exchange where H^+ displaces charge-balancing cations (M^{n+}, M = Na^+, K^+, Ca^{2+}) in the Si–O–Al network, supported by EDS and FTIR evidence. Formula 3 indicates gypsum formation ($CaSO_4 \cdot 2H_2O$) from leached Ca^{2+}, confirmed by deposits in Fig. 11a and the sulphur detection in Table 7. Formula 4 summarises the three-stage degradation pathway. Formula 5 compares the control and bio-modified outcomes, where less leaching and better Ca/Fe retention improve matrix integrity, supported by molar ratio and XRD data.

Acid dissociation:

$$H_2SO_4 \rightarrow 2H^+ + SO_4^{2-} \quad (1)$$

Ion exchange/leaching:

$$(Si - O - AI - M) + H^+ \rightarrow Si - OH + AI - OH + M^{n+} \quad (2)$$

Sulphate product formation:

$$Ca^{2+} + SO_4^{2-} + 2H_2O \rightarrow CaSO_4 \cdot 2H_2O \quad (3)$$

Overall degradation pathway:

$$\text{Acid attack} \rightarrow \text{ion exchange} \rightarrow \text{leaching} \rightarrow \text{porosity} \rightarrow \text{weakening} \quad (4)$$

Bio-modified response:

$$\text{Reduced leaching} + \text{Ca/Fe retention} \rightarrow \text{better matrix integrity} \quad (5)$$

M=Na, K, Ca

5 Conclusion

The present study confirms that Shewanella oneidensis species-based bio-modification significantly enhances the durability of fly ash-based geopolymer concrete under sulphuric acid exposure, affirming its potential for sewer infrastructure applications.

In terms of mechanical performance, bio-modified specimens exhibited consistently lower mass loss, resistance to gypsum-related mass gain, and an 82% increase in splitting tensile strength following acid exposure, contrasting with a 13% decrease recorded in control specimens. Reduced post-acid exposure water absorption further supports enhanced microstructural density and diminished porosity in bio-modified matrices, attributed to bacterially mediated $CaCO_3$ precipitation and matrix densification.

Microstructural and mineralogical analyses corroborate these findings. SEM–EDS confirmed reduced cracking and enhanced retention of Fe, O, and Ca in bio-modified specimens, consistent with the formation of stable phases, notably andradite. XRD demonstrated the retention of quartz, albite, and anorthite in bio-modified samples alongside andradite formation, indicating reduced depolymerisation and preserved gel structure, whereas control samples showed greater phase degradation and decalcification. FTIR analysis revealed enhanced Si–O–T bond retention in bio-modified specimens, reflecting a more intact aluminosilicate framework, while elevated Ca/Al and Fe/Al molar ratios confirmed superior retention of structural elements under acidic conditions.

These results endorse the application of Shewanella species-based bio-modified geopolymer concrete in aggressive sewer environments. Future research will evaluate long-term performance under varying pH, temperature, humidity, and cyclic wet-dry regimes, examining the influence of sewer exposure conditions on bacterial metabolic activity and healing efficiency. Complementary life cycle assessments (LCA) and cost–benefit analyses, including embodied CO_2 metrics, will assess the environmental and economic feasibility of bio-modified geopolymer concrete for sewer infrastructure.

Acknowledgements We would like to express our deep gratitude to the UKRI for the support of the Horizon Europe Horizon MSCA Postdoctoral Fellowship 2022 EP/Y015959/1, Alternative Biomineralisation for Concrete without cement (ABioC).

Author contribuitons Mehrdad Ameri Vamkani: Conceptualisation, Formal analysis, Investigation, Writing—original draft. Zarina Yahya: Investigation, Formal analysis, Writing—review & editing. Michaela Gkantou: Writing—review & editing, Supervision. Maria Ferentinou: Writing—review & editing, Supervision. Yangming Gao: Writing—review & editing, Supervision. Ana Bras: Conceptualisation, Methodology, Formal analysis, Validation, Writing—original draft, Funding, Writing—review & editing, Supervision.

Funding HORIZON EUROPE Marie Sklodowska-Curie Actions,EP/Y015959/1,Ana Bras

Data availability Data will be available upon request.

Declarations

Conflict of interest The authors declare that they have no known competing financial interests or personal relationships that could have appeared to influence the work reported in this paper.

Appendix A

Supplementary SEM–EDS elemental maps

Figure 15 presents the SEM–EDS elemental distribution maps for potassium (K), magnesium (Mg), and titanium (Ti) in geopolymer specimens at 180 days. These elements were detected in both control and bio-modified specimens but are not directly implicated in the primary degradation or bio-modification mechanisms discussed in Sects. 4.6.3–4.9. They are included here for completeness and to provide a full elemental characterisation of the geopolymer matrix.

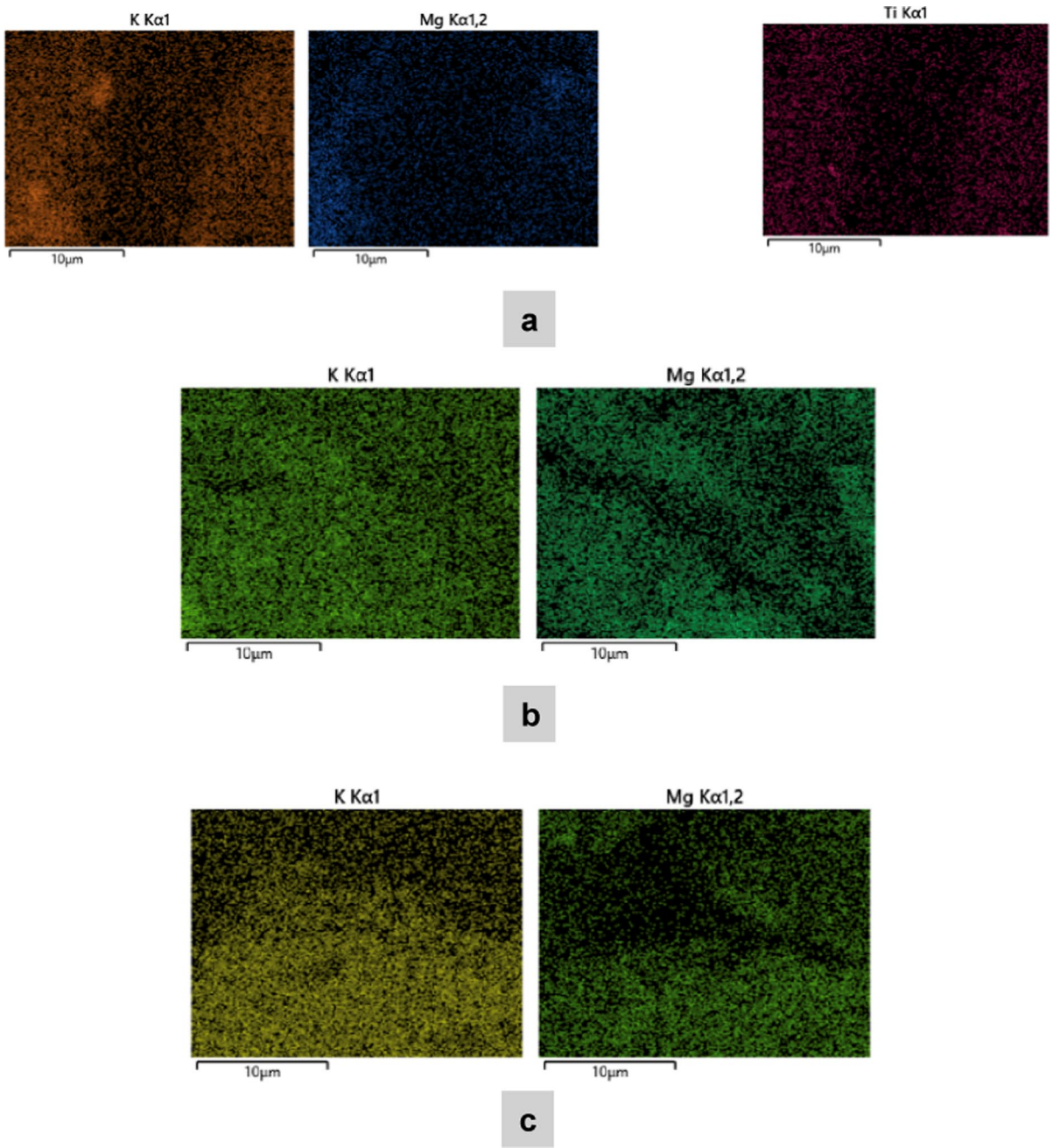

Fig. 15 SEM–EDS elemental maps showing the spatial distribution of potassium (K), magnesium (Mg), and titanium (Ti) at 180 days in: **a** bio-modified specimen without acid exposure, **b** control specimen without acid exposure, **c** bio-modified specimen with 10-day acid exposure

References

1. Guo X, Yuan S, Liu X (2023) The self-healing properties and mechanism of the cracked fly ash-based engineered geopolymer composites (FA-EGC): effects of water and temperature. J Sustain Cem-Based Mater 12(10):1228–1241. https://doi.org/10.1080/21650373.2023.2213227
2. Khan I, Xu T, Castel A, Gilbert RI, Babaee M (2019) Risk of early age cracking in geopolymer concrete due to restrained shrinkage. Constr Build Mater 229:116840. https://doi.org/10.1016/j.conbuildmat.2019.116840
3. Zhao D, Li K, Li Y, Chen X, Fan J, Zhu J (2024) Self-healing behaviour of fly ash/slag-based engineered geopolymer composites under external alkaline environments. Case Stud Constr Mater 21:e03361. https://doi.org/10.1016/j.cscm.2024.e03361
4. Shams H, Hayat S, Ullah H, Abdrhman H, Qiu Y (2024) Alkali-Silica potential in fly-ash-based geopolymer concrete. Mater Struct 57(9):192. https://doi.org/10.1617/s11527-024-02479-8
5. Kanagaraj B, Kiran T, Anand N, Jayakumar G, Lubloy E (2025) Bamboo reinforced panels with recycled concrete aggregates: A comparative study between cement and geopolymer concrete. Dev Built Environ 24:100753. https://doi.org/10.1016/j.dibe.2025.100753
6. Bakera AT, Alexander MG (2024) In situ concrete sewer performance: comparison of Portland cement, calcium sulfoaluminate cement, and calcium aluminate cement. Mater Struct 57(5):114. https://doi.org/10.1617/s11527-024-02390-2
7. Grengg C, Mittermayr F, Ukrainczyk N, Koraimann G, Kienesberger S, Dietzel M (2018) Advances in concrete materials for sewer systems affected by microbial induced concrete corrosion: A review. Water Res 134:341–352. https://doi.org/10.1016/j.watres.2018.01.043
8. Bakera AT, Damion T, Alexander M, Chaunsali P (2025) Biogenic acid attack of portland cement: reactive transport modelling, laboratory studies, and field observations of effect of different pH. Mater Struct 58(10):357. https://doi.org/10.1617/s11527-025-02878-5
9. Roviello G et al (2025) Geopolymer-based composite and hybrid materials: The synergistic interaction between components. Sustain Mater Technol 44:e01404. https://doi.org/10.1016/j.susmat.2025.e01404
10. Maradani LSR, Pradhan B (2025) Influence of aggressive agents on properties of geopolymer concrete and corrosion behavior of steel in geopolymer concrete pore solution. Mater Struct 58(4):102. https://doi.org/10.1617/s11527-025-02633-w
11. Chen Z, Yu J, Nong Y, Yang Y, Zhang H, Tang Y (2023) Beyond time: enhancing corrosion resistance of geopolymer concrete and BFRP bars in seawater. Compos Struct 322:117439. https://doi.org/10.1016/j.compstruct.2023.117439
12. Caicho-Caranqui J et al (2025) Towards sustainable bio-plasticizers from biomass to polymers applications: A review. Sustain Mater Technol 43:e01194. https://doi.org/10.1016/j.susmat.2024.e01194
13. Grengg C, Ukrainczyk N, Koraimann G, Mueller B, Dietzel M, Mittermayr F (2020) Long-term *in situ* performance of geopolymer, calcium aluminate and Portland cement-based materials exposed to microbially induced acid corrosion. Cem Concr Res 131:106034. https://doi.org/10.1016/j.cemconres.2020.106034
14. Sa Ribeiro RA, Sa Ribeiro MG, Samuel DM, Ozer A, Numkiatsakul P, Kriven WM (2025) Metakaolin-based geopolymer matrix formulations for higher strength and thermal stability'. Mater Struct 58(4):142. https://doi.org/10.1617/s11527-025-02670-5
15. Yao S et al (2025) Preparation of coal gangue-based one-part geopolymers using solid activators with different Al/Si ratios. J Build Eng 111:113583. https://doi.org/10.1016/j.jobe.2025.113583
16. Garces JIT, Tan RR, Beltran AB, Ongpeng JMC, Promentilla MAB (2021) Environmental life cycle assessment of alkali-activated material with different mix designs and self-healing agents. Chem Eng Trans 88:835–840. https://doi.org/10.3303/CET2188139
17. Luhar S, Luhar I, Shaikh FUA (2021) Review on performance evaluation of autonomous healing of geopolymer composites. Infrastructures. https://doi.org/10.3390/infrastructures6070094
18. Mohammed H, Ortoneda-Pedrola M, Nakouti I, Bras A (2020) Experimental characterisation of non-encapsulated bio-based concrete with self-healing capacity. Constr Build Mater 256:119411. https://doi.org/10.1016/j.conbuildmat.2020.119411
19. Bagga M et al (2023) Assessing the potential application of bacteria-based self-healing cementitious materials for enhancing durability of wastewater treatment infrastructure. Cem Concr Compos 143:105259. https://doi.org/10.1016/j.cemconcomp.2023.105259
20. Zhang H, Kumar Sarker P, Wang Q, He B, Chandra Kuri J, Jiang Z (2023) Comparison of compressive, flexural, and temperature-induced ductility behaviours of steel-PVA hybrid fibre reinforced OPC and geopolymer concretes after high temperatures exposure. Constr Build Mater 399:132560. https://doi.org/10.1016/j.conbuildmat.2023.132560
21. Amran M et al (2021) Long-term durability properties of geopolymer concrete: An in-depth review. Case Stud Constr Mater 15:e00661. https://doi.org/10.1016/j.cscm.2021.e00661
22. Elmenshawy Y, Elmahdy MAR, Moawad M, Elshami AA, Ahmad SSE, Nagai K (2024) Investigating the bacterial sustainable self-healing capabilities of cracks in structural concrete at different temperatures. Case Stud Constr Mater 20:e03188. https://doi.org/10.1016/j.cscm.2024.e03188
23. Snoeck D, De Belie N (2025) Evaluation of self-healing crack repair sticks for enhanced durability, sealing, and stiffness recovery of concrete. Dev Built Environ 23:100712. https://doi.org/10.1016/j.dibe.2025.100712

24. Cappellesso VG, Van Mullem T, Gruyaert E, Van Tittelboom K, De Belie N (2024) Self-healing concrete with a bacteria-based or crystalline admixture as healing agent to prevent chloride ingress and corrosion in a marine environment. Dev Built Environ 19:100486. https://doi.org/10.1016/j.dibe.2024.100486
25. Sarkar M, Maiti M, Mandal S, Xu S (2024) Enhancing concrete resilience and sustainability through fly ash-assisted microbial biomineralization for self-healing: From waste to greening construction materials. Chem Eng J 481:148148. https://doi.org/10.1016/j.cej.2023.148148
26. Chatterjee A, Alam N, Chowdhury T, Chattopadhyay B (2024) Modified bacteria incorporated geopolymer - a qualitative approach for an eco-friendly, energy-efficient and self-healing construction material. J Civil Eng Construc. https://doi.org/10.32732/jcec.2024.13.1.44
27. Van Tittelboom K, De Belie N, De Muynck W, Verstraete W (2010) Use of bacteria to repair cracks in concrete. Cem Concr Res 40(1):157–166. https://doi.org/10.1016/j.cemconres.2009.08.025
28. Singh VK, Srivastava G (2024) Development of a sustainable geopolymer using blast furnace slag and lithium hydroxide. Sustain Mater Technol 40:e00934. https://doi.org/10.1016/j.susmat.2024.e00934
29. Wang Y, Liu H, Nie Z, Xue R, Zhu W, Sun X (2025) Experimental investigation into the influence of calcium aluminate cement on the micro- and macro-mechanical properties of the interfacial transition zone in geopolymer concrete. Dev Built Environ 21:100618. https://doi.org/10.1016/j.dibe.2025.100618
30. Kanagaraj B, Anand N, Lubloy E (2024) Sustainability and durability performance evaluation of geopolymer concrete with industrial effluent as alternative to conventional river sand. Dev Built Environ 19:100517. https://doi.org/10.1016/j.dibe.2024.100517
31. Yang Z et al (2024) Synthesis of eco-sustainable seawater sea-sand geopolymer mortars from ternary solid waste: influence of microstructure evolution on mechanical performance. Sustain Mater Technol 41:e01056. https://doi.org/10.1016/j.susmat.2024.e01056
32. Yu Y, Al-Damad IMA, Foster S, Nezhad AA, Hajimohammadi A (2025) Compressive strength prediction of fly ash/slag-based geopolymer concrete using EBA-optimised chemistry-informed interpretable deep learning model. Dev Built Environ 23:100736. https://doi.org/10.1016/j.dibe.2025.100736
33. Kanagaraj B, Samuvel Raj R, Anand N, Lubloy E (2025) Engineering and sustainability performance of geopolymer concrete blended with sodium silicate effluent. Dev. Built Environ. 22:100678. https://doi.org/10.1016/j.dibe.2025.100678
34. Rihan MAM, Alahmari TS, Onchiri RO, Gathimba N, Sabuni B (2024) Impact of alkaline concentration on the mechanical properties of geopolymer concrete made up of fly ash and sugarcane bagasse ash. Sustainability. https://doi.org/10.3390/su16072841
35. Wu J-Q, Li B, Chen Y-T, Shi W, Ghiassi B (2024) Self-healing performance of engineered geopolymer composites subjected to sodium sulphate. J Build Eng 97:110789. https://doi.org/10.1016/j.jobe.2024.110789
36. Abir AH (2026) Engineered microbial self-healing strategies in low-carbon concrete: A critical review. Mater 10:101443. https://doi.org/10.1016/j.nxmate.2025.101443
37. Madirisha MM, Dada OR, Ikotun BD (2024) Chemical fundamentals of geopolymers in sustainable construction. Mater Today Sustain 27:100842. https://doi.org/10.1016/j.mtsust.2024.100842
38. Fredrickson JK et al (2008) Towards environmental systems biology of Shewanella. Nat Rev Microbiol 6(8):592–603. https://doi.org/10.1038/nrmicro1947
39. Hau HH, Gralnick JA (2007) Ecology and biotechnology of the genus *Shewanella*. Annu Rev Microbiol 61(1):237–258. https://doi.org/10.1146/annurev.micro.61.080706.093257
40. Perez-Gonzalez T et al (2010) Magnetite biomineralization induced by Shewanella oneidensis. Geochim Cosmochim Acta 74(3):967–979. https://doi.org/10.1016/j.gca.2009.10.035
41. Doostkami H, De Jesús Estacio J, Cumberbatch S, Formagini PS, Roig-Flores M (2023) Self-healing capability of conventional, high-performance, and ultra high-performance concrete with commercial bacteria characterized by means of water and chloride penetration'. Constr Build Mater 401:132903. https://doi.org/10.1016/j.conbuildmat.2023.132903
42. N. M. Apandi et al (2024) Optimization of Alkali Activator on the Strength Properties of Fly Ash Based Geopolymer Repair Materials, Arch. Metall. Mater. 69(1): 5–8 Accessed: Apr. 04, 2025. [Online]. Available: https://journals.pan.pl/dlibra/publication/147775/edition/130872
43. Naresh T, Mallik M, R S V, Madduru SRC, Nandipati S (2024) Influence of activator solution and binder composition on the characteristics of self-compacting geopolymer concrete. Civ Eng Archit 12(3):1526–1539. https://doi.org/10.13189/cea.2024.120320
44. Bernal SA, Rodríguez ED, Mejía De Gutiérrez R, Provis JL (2012) Performance of alkali-activated slag mortars exposed to acids. J Sustain Cem-Based Mater 1(3):138–151. https://doi.org/10.1080/21650373.2012.747235
45. Grengg C et al (2021) Deterioration mechanism of alkali-activated materials in sulfuric acid and the influence of Cu: a micro-to-nano structural, elemental and stable isotopic multi-proxy study. Cem Concr Res 142:106373. https://doi.org/10.1016/j.cemconres.2021.106373
46. Luhar I, Luhar S (2022) A comprehensive review on fly ash-based geopolymer. J Compos Sci 6(8):219. https://doi.org/10.3390/jcs6080219
47. Vafaei M, Allahverdi A (2017) Durability of geopolymer mortar based on waste-glass powder and calcium aluminate cement in acid solutions. J Mater Civ Eng 29(10):04017196. https://doi.org/10.1061/(ASCE)MT.1943-5533.0002053
48. S. Wallah and B. Rangan (2025) Low-Calcium fly ash-based geopolymer concrete: Long-term properties' Accessed: Apr. 04, 2025. [Online]. Available: https://www.semanticscholar.org/paper/Low-Calcium-fly-ash-based-geopolymer-concrete%3A-Wallah-Rangan/6645bf919ea25428adadedd44b213fe8a39d5568
49. K. Mukilan, R. Ilayarsi, S. K. Kumar, M. Abhinayan, C. Sathyanarayanan, and K. Vilwanathan, (2024) Effect

of mineral admixtures on the performance of self-compacting geopolymer concrete, E3S Web Conf 529 01022 https://doi.org/10.1051/e3sconf/202452901022.
50. Adeleke BO, Kinuthia JM, Oti J, Pirrie D, Power M (2024) Mechanical and microstructural investigation of geopolymer concrete incorporating recycled waste plastic aggregate. Materials. https://doi.org/10.3390/ma17061340
51. Zeng J, Zhang K, Sun W, Zeng Y, Zou Z (2024) Mechanics and microstructure analysis of geopolymer utilizing ilmenite tailing and metakaolin powder as alkali-activated materials. Case Stud Constr Mater 21:e03567. https://doi.org/10.1016/j.cscm.2024.e03567
52. Yuan L et al (2022) Orthogonal analysis and mechanism of compressive strength and microstructure of the metakaolin-fly ash geopolymer. Case Stud Constr Mater 17:e01154. https://doi.org/10.1016/j.cscm.2022.e01154
53. Bras A, Mohammed H, Romano A, Nakouti I (2022) Biomineralisation to increase earth infrastructure resilience. Materials (Basel) 15(7):2490. https://doi.org/10.3390/ma15072490
54. Fu L, Li S-W, Ding Z-W, Ding J, Lu Y-Z, Zeng RJ (2016) Iron reduction in the DAMO/*Shewanella oneidensis* MR-1 coculture system and the fate of Fe(II). Water Res 88:808–815. https://doi.org/10.1016/j.watres.2015.11.011
55. Ariyadasa PW, Manalo AC, Lokuge W, Aravienthan V, Gerdes A, Kaltenbach J (2025) Degradation mechanisms of low-calcium fly ash-based geopolymer mortar in simulated aggressive sewer conditions. Cem Concr Res 194:107882. https://doi.org/10.1016/j.cemconres.2025.107882
56. Javed U, Shaikh FUA, Sarker PK (2024) Corrosive effect of HCl and H2SO4 exposure on the strength and microstructure of lithium slag geopolymer mortars. Constr Build Mater 411:134588. https://doi.org/10.1016/j.conbuildmat.2023.134588
57. Liu J, Doh J-H, Dinh HL, Ong DEL, Zi G, You I (2022) Effect of Si/Al molar ratio on the strength behavior of geopolymer derived from various industrial waste: a current state of the art review. Constr Build Mater 329:127134. https://doi.org/10.1016/j.conbuildmat.2022.127134
58. Dinh HL, Liu J, Doh J-H, Ong DEL (2024) Influence of Si/Al molar ratio and ca content on the performance of fly ash-based geopolymer incorporating waste glass and GGBFS. Constr Build Mater 411:134741. https://doi.org/10.1016/j.conbuildmat.2023.134741
59. Wang H, Wu H, Xing Z, Wang R, Dai S (2021) The effect of various Si/Al, Na/Al molar ratios and free water on micromorphology and macro-strength of metakaolin-based geopolymer. Materials (Basel) 14(14):3845. https://doi.org/10.3390/ma14143845
60. Bai Y et al (2023) Performance deterioration of municipal solid waste incineration fly ash-based geopolymer under sulfuric acid attack. Constr Build Mater 391:131847. https://doi.org/10.1016/j.conbuildmat.2023.131847
61. Yang W, Zhu P, Liu H, Wang X, Ge W, Hua M (2021) Resistance to sulfuric acid corrosion of geopolymer concrete based on different binding materials and alkali concentrations. Materials (Basel) 14(23):7109. https://doi.org/10.3390/ma14237109
62. Gevaudan JP, Santa-Ana B, Srubar WV (2021) Iron mineral admixtures improve the sulfuric acid resistance of low-calcium alkali-activated cements. Cem Concr Compos 116:103867. https://doi.org/10.1016/j.cemconcomp.2020.103867
63. El Alouani M et al (2024) A comprehensive review of synthesis, characterization, and applications of aluminosilicate materials-based geopolymers. Environ Adv 16:100524. https://doi.org/10.1016/j.envadv.2024.100524
64. Ajay A, Ramaswamy KP, Thomas AV (2020) A critical review on the durability of geopolymer composites in acidic environment. IOP Conf Ser Earth Environ Sci 491(1):012044. https://doi.org/10.1088/1755-1315/491/1/012044
65. Benavent V, Lahalle H, Patapy C, Renaudin G, Cyr M (2022) Microstructural evolution of a sodium metakaolin-based geopolymer paste in neutral and CEM V basic environment. Cem Concr Res 161:106897. https://doi.org/10.1016/j.cemconres.2022.106897